Project Update: Flow and Heat Transfer Characterization of Lean Pre-mixed Combustor Systems

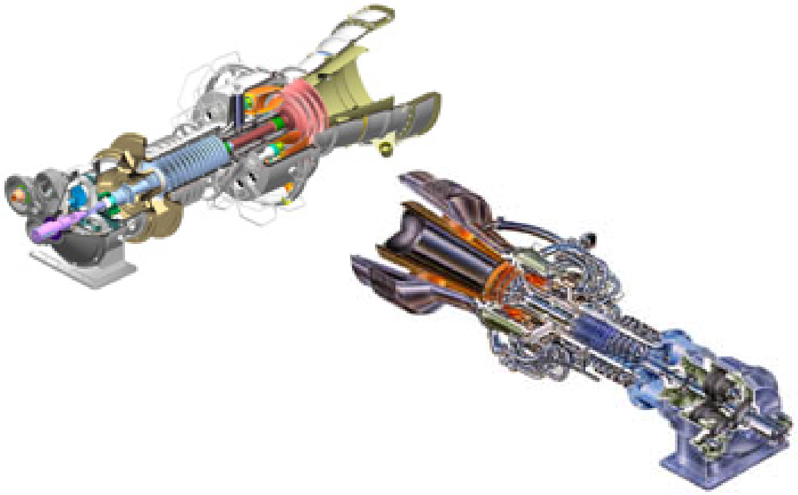

Taurus 65 and Taurus 70 Turbines
Courtesy of Solar Turbines Inc.

Presented by:
Srinath V. Ekkad, PhD.
Suhyeon Park
Siddhartha Gadiraju

Project sponsored by:
Department of Energy
Solar Turbines, Inc.

VirginiaTech
Invent the Future®

APPL

Virginia Tech - Combustion Team

Prof. Srinath V. Ekkad (Moved to NCSU - Sep. 2017)
- Principal investigator
- Rolls-Royce professor, Mechanical Engineering Dept.
- Associate Vice-President of Research at Virginia Tech

David Gomez-Ramirez (Graduated - Jul. 2016)
- Ph.D in Mechanical Engineering
- Current Affiliation : Schlumberger
- Thermofluids system design and advanced measurements

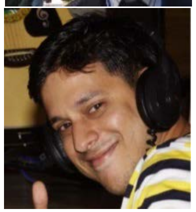

Sandeep Kedukodi (Graduated - May. 2017)
- Ph.D student in Mechanical Engineering
- M.S in Mechanical Engineering, Birla Institute of Technology, Ranchi, India
- Current research : Computational investigations of flow and heat transfer

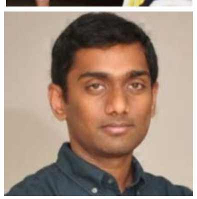

Siddhartha Gadiraju
- Ph.D student in Mechanical Engineering
- M.S in Mechanical Engineering, Stony Brook University
- Current research : Experiment in combustion instability, heat transfer

Suhyeon Park
- Ph.D student in Mechanical Engineering
- M.S in Mechanical Engineering, KAIST, Korea
- Current research : Experiment in flow field and heat transfer measurement

Yongbin Ji (Went back to China - Sep. 2017)
- Visiting scholar from Shanghai Jiao Tong University, China (PhD student)
- Experience: Experimental investigation on flow field and cooling of effusion cooled multi-nozzle combustor

Optical Combustor Rig

Updates on combustor test rig at Virginia Tech

Optical Combustor Rig Features

Features:

- Industrial nozzle testing
- Air flow 2.8 lbm/s at 150 psig
- Flow metering 2% accuracy, 0.25% repeatable
- 192 kW inline heater

Flexibility:

- Outlet geometries, dome assemblies, swirl fuel nozzles, liners.

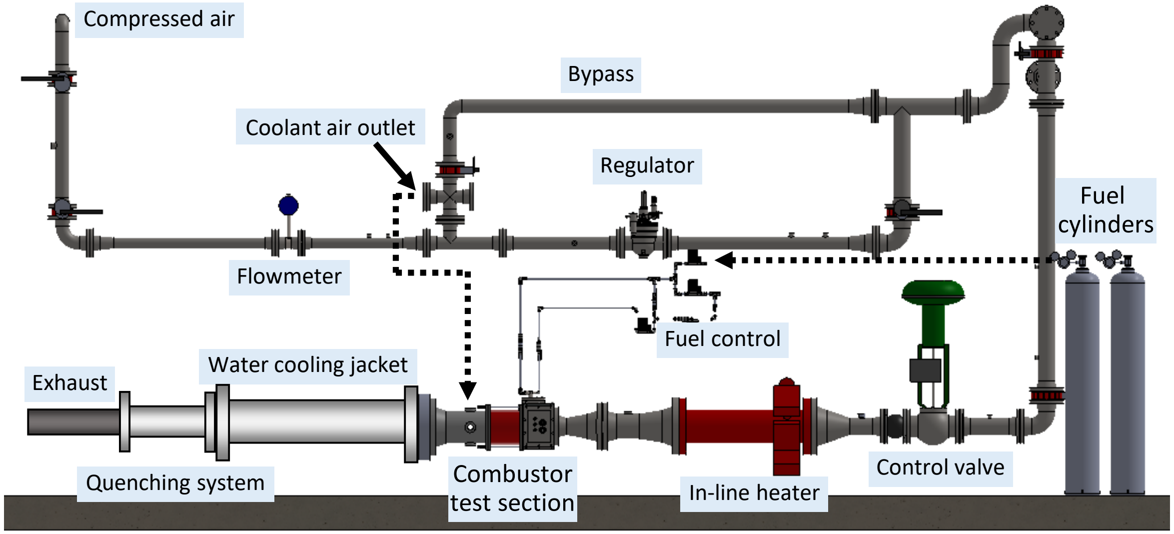

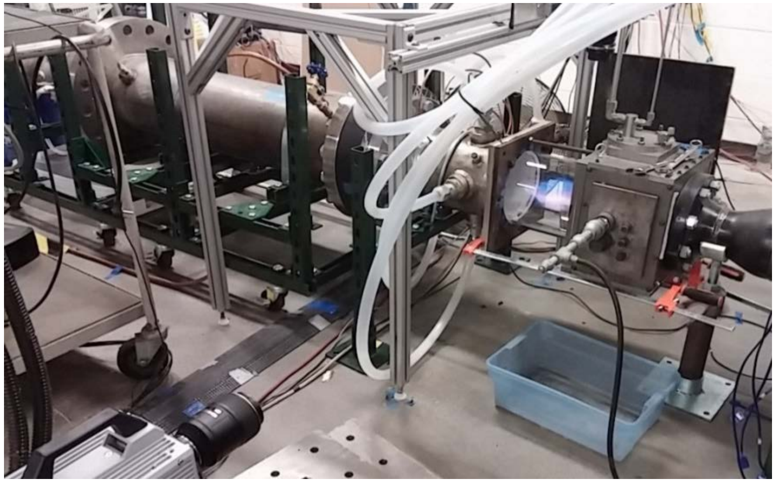

Optical access for flame diagnostics and liner/fuel nozzle evaluation:

- PIV and IR thermography.
- Potential for absorption measurements, Laser Induced Fluorescence (LIF), thermographic phosphors.

Axial swirl type premixed fuel nozzle

Industrial fuel nozzle

by Solar Turbines Inc.

Input ports

- Air

  Small % to pilot nozzle

  Most to main nozzle
- Main fuel
- Pilot fuel

Output ports

- Main nozzle: air + main nozzle
- Pilot nozzle: air + pilot nozzle

Features

- Overall fuel air ratio

  = (main fuel + pilot fuel)/(total air)
- Pilot flow increases stability

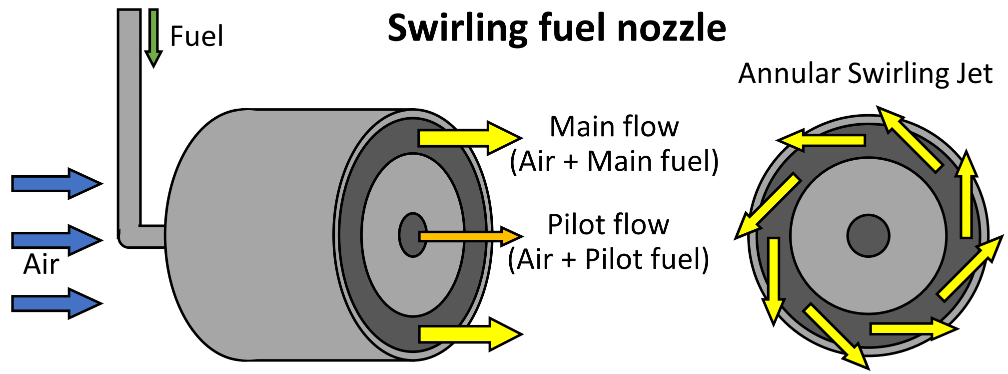

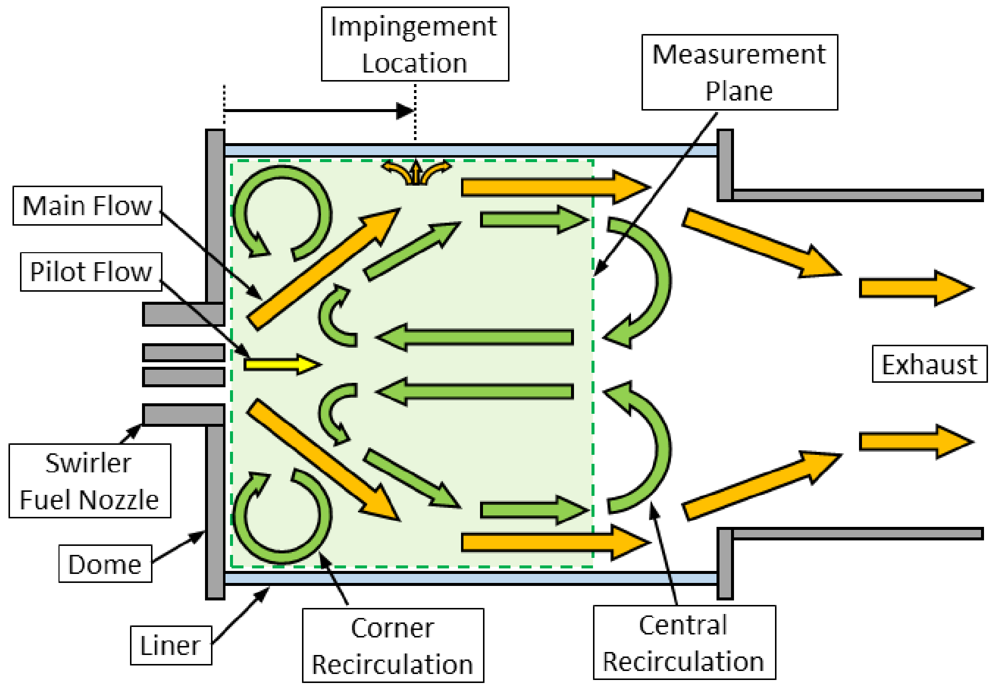

Rig Upgrade – Test section

Added parts

- Exhaust connection
  - ✓ Transition piece
  - ✓ Water cooled jacketed pipe
  - ✓ Quenching system
- Double liner add-on piece
- Integrated dome plate
  - ✓ Air-cooling
  - ✓ Pressure transducer
  - ✓ Thermocouple
  - ✓ Built-in ignition

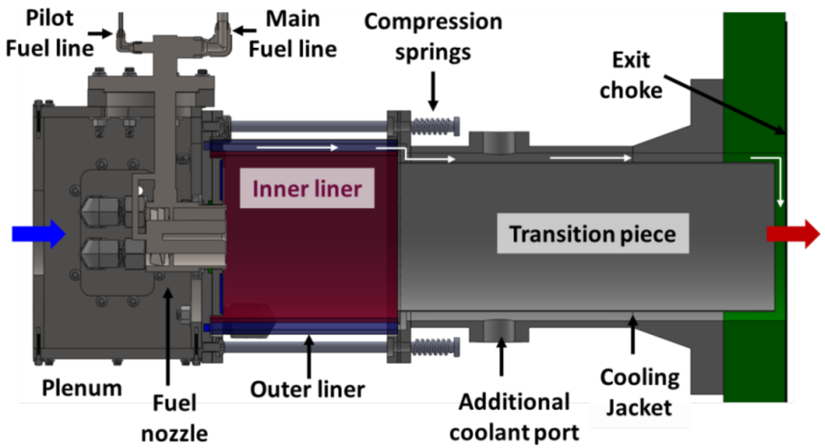

Closed test section with double liner

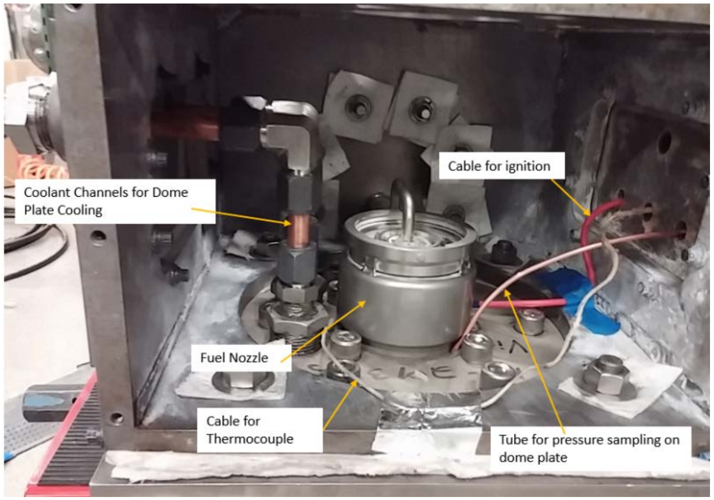

Inside of settling chamber

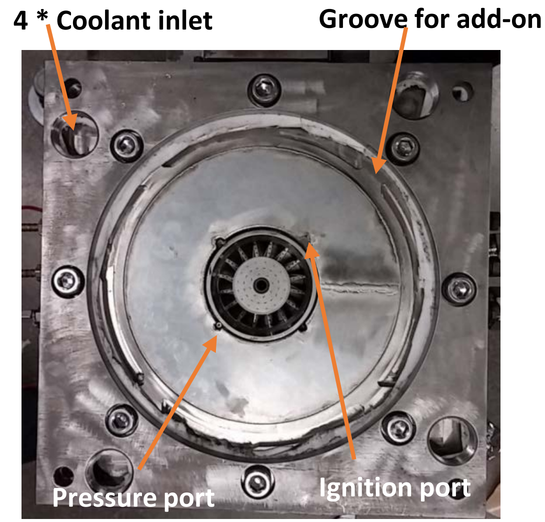

New dome plate

Rig Upgrade – Control and acquisition

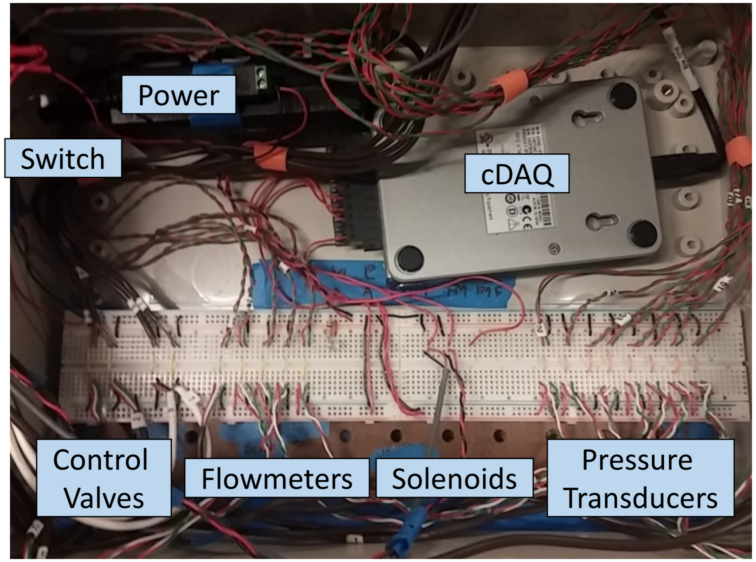

Electrical box connections

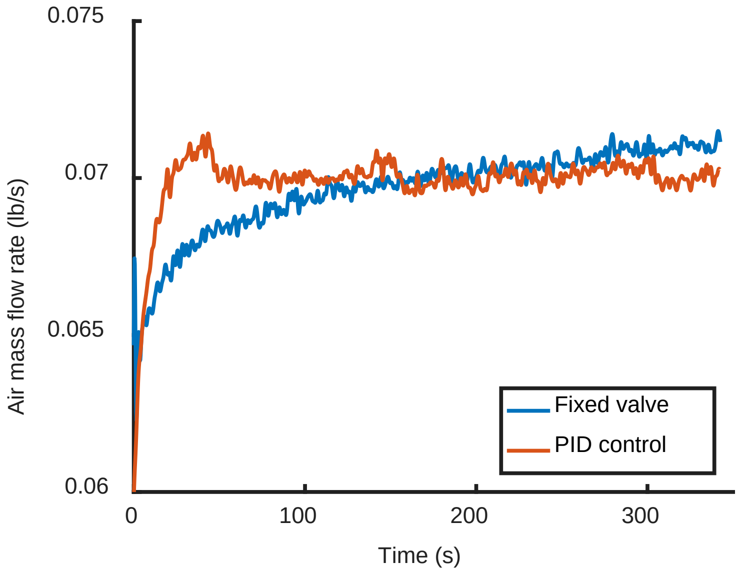

PID Control

Upgradation of the control and acquisition system

- Flow rate drift was removed by PID control
  Peak-to-peak error was reduced from 4.3% to 1.4 % (0.003 to 0.001 lb/s)
- DAQ upgrade to PXI system
- Wire connections are re-organized in an electrical box
- Integrated LabVIEW control

Rig Upgrade – Fuel supply system

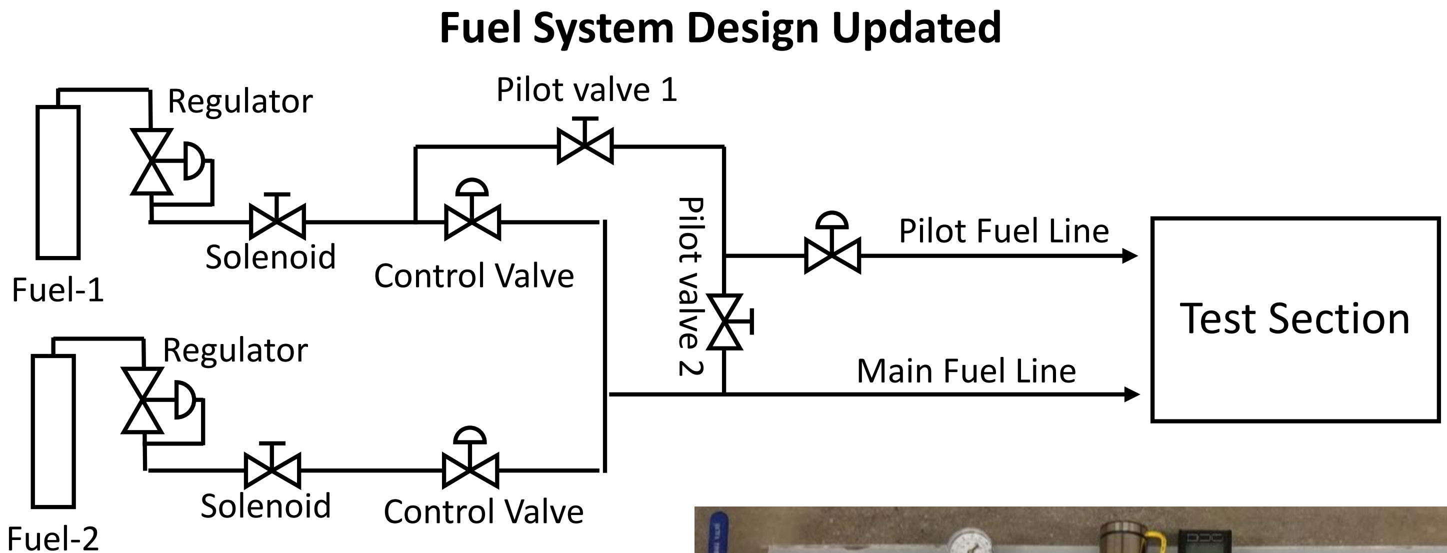

- Control valves:
  Alicat mass flow controllers
  - Fast, precise measurement and control
  - Mass flowmeter + control
  - Max P : 145 psig

Liner Wall Heat Transfer

Non-intrusive infrared thermographic camera measurement on reacting combustor

Combustor liner heat transfer

Previous work validated the technique

Goal

- Investigate interaction between flow field and heat transfer on the liner wall
- Compare heat transfer characteristics on combustor liner with PIV flow field inside liner

Liner wall coating

- black paint spray, 5 coats
  - Inner wall coat : whole area in the view
  - Outer wall coat : a section in the view

Combustor operating condition

- Re 50k, ϕ = 0.65, pilot 6-7%
- Geometry: Closed combustor downstream (previously done with open combustor)

Measurement setup

- FLIR SC6700 + KG2 filter glass
- Frame rate: 5 Hz rate
- Duration: ~180 s

SC6700 + KG2

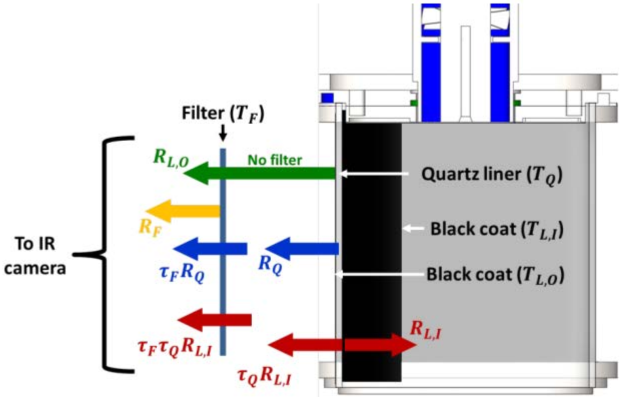

Top view schematic

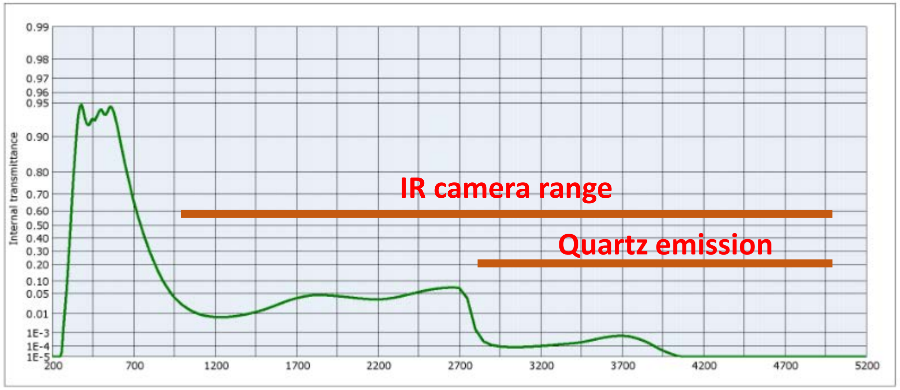

Time-Dependent, Non-Intrusive IR Measurement

IR camera to measure inner and outer **surface temperature**

↓

Boundary conditions in a finite difference model of the liner

↓

Calculate **heat flux into the liner** from the normal temperature gradient

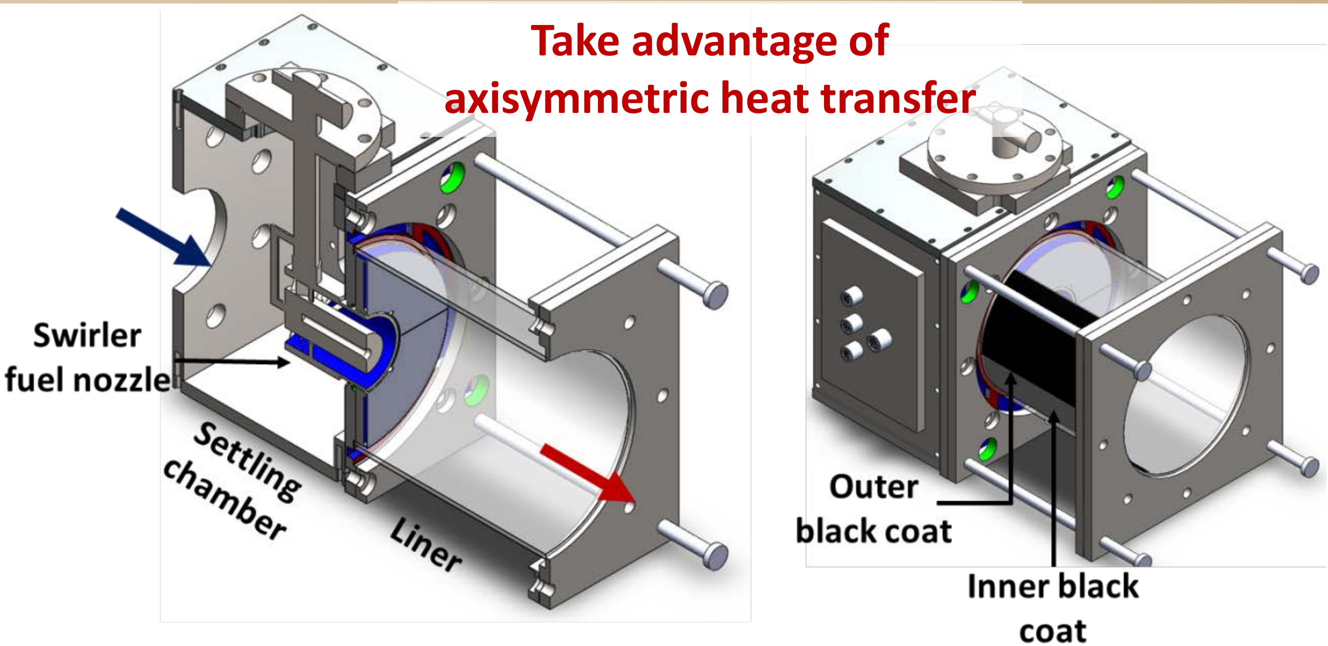

Heat conduction equation for the quartz liner

$$\rho C_p \frac{\partial T}{\partial t} = \frac{\partial}{\partial x}\left(k\frac{\partial T}{\partial x}\right) + \frac{1}{r}\frac{\partial}{\partial r}\left(kr\frac{\partial T}{\partial r}\right)$$

Energy balance at the inner surface

$$-k\frac{\partial T}{\partial r}_{r=r_0} = h\left(T_{r=r_0} - T_\infty\right)$$

Inner and outer wall temperature measured in time

Combustor set point
- Re : 50 k
- ϕ : 0.65
- Pilot: 6%

Measurement
- FLIR SC6700
- Fps : 5 Hz
- KG2 filter
- Duration: 180 s

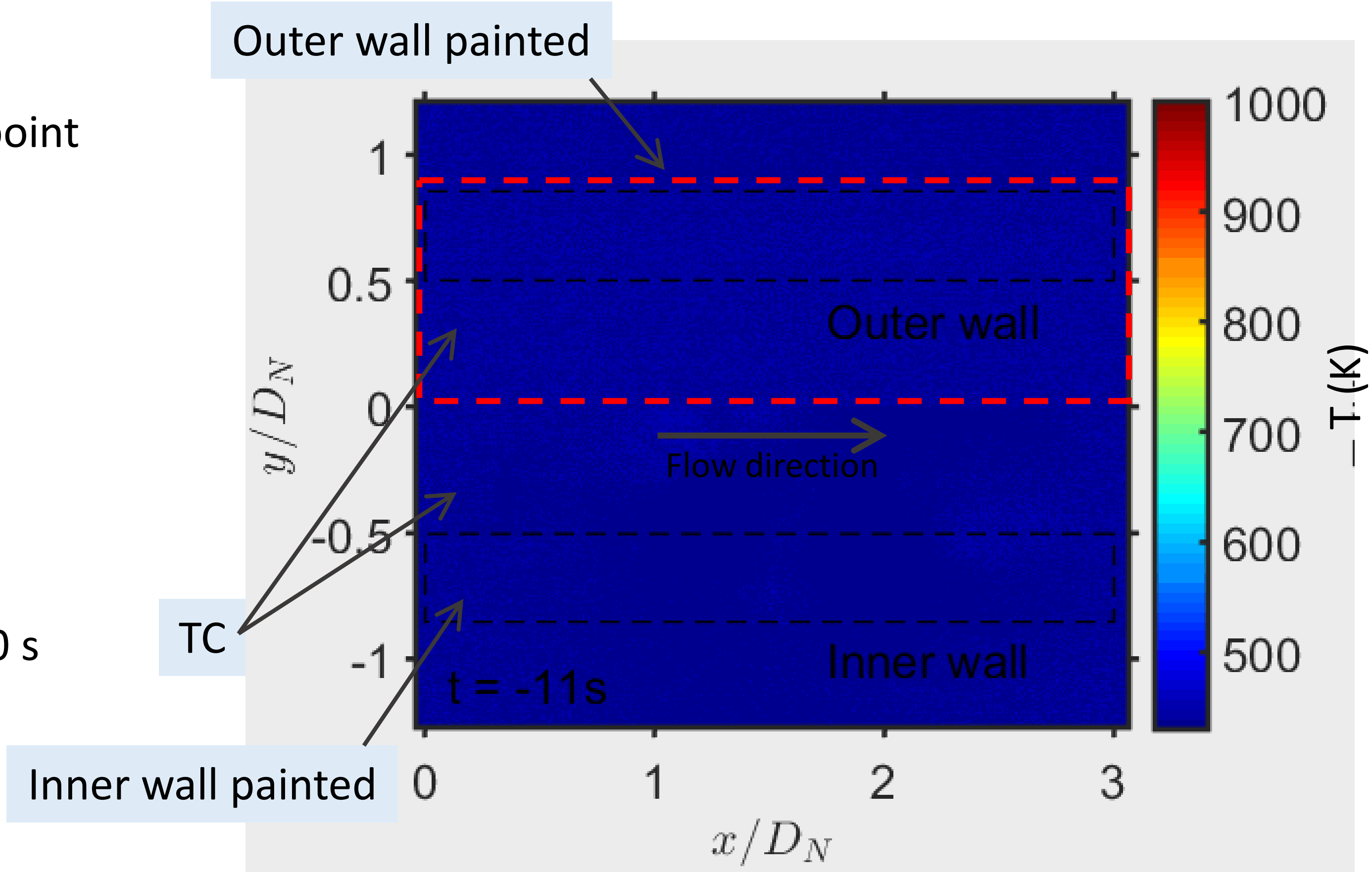

- Calibrated temperature of inner and outer liner surface
- Pilot flame was on at t<0, Main flame started at t=0

Liner wall temperature axial profile

Time dependent liner temperature profiles

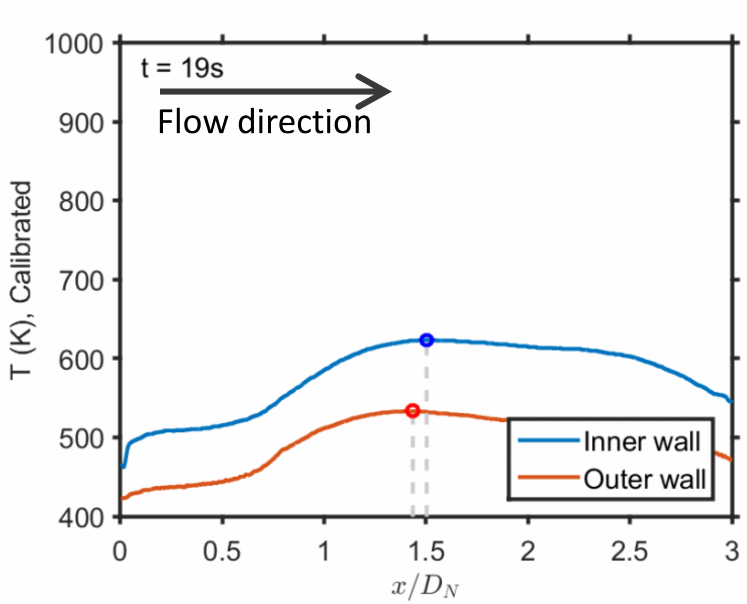

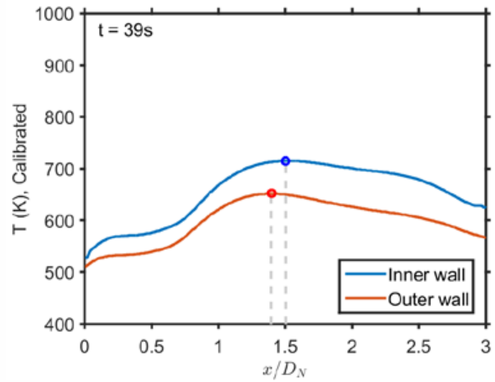

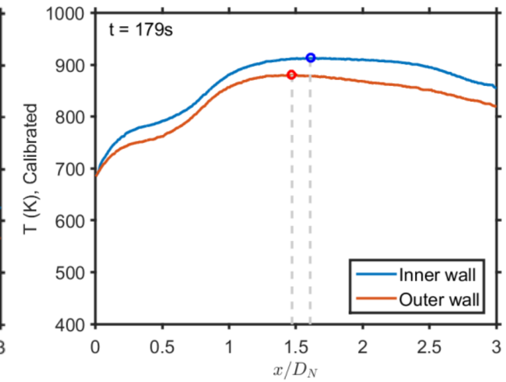

- Peak temperature location found at x = 1.5 D_N from the fuel nozzle
- Maximum measured temperature :
  - 912 K (639 C) at inner wall
  - 880 K (607 C) at outer wall

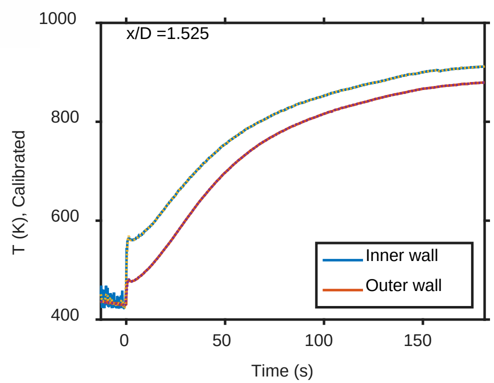

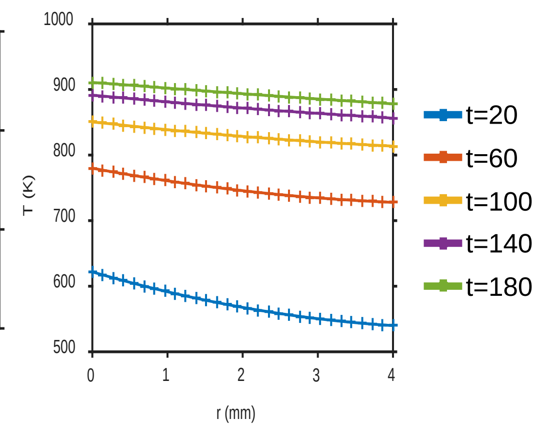

Combustor liner heat flux measurement

- High heat transfer at low liner temperature
- Peak location moves downstream, from *x/D* = 1.8 (*t*=20) to *x/D* = 2.4 (*t*=180)
- Heat transfer at steady state at *t* > 160
- Heat transfer peak is 23 kW/m2 at $x/D_N \approx 2.3$ at steady state
- Increase of heat flux at $0.9 \leq x/D_N \leq 2.3$ due to heat release in reacting flow attached to liner wall

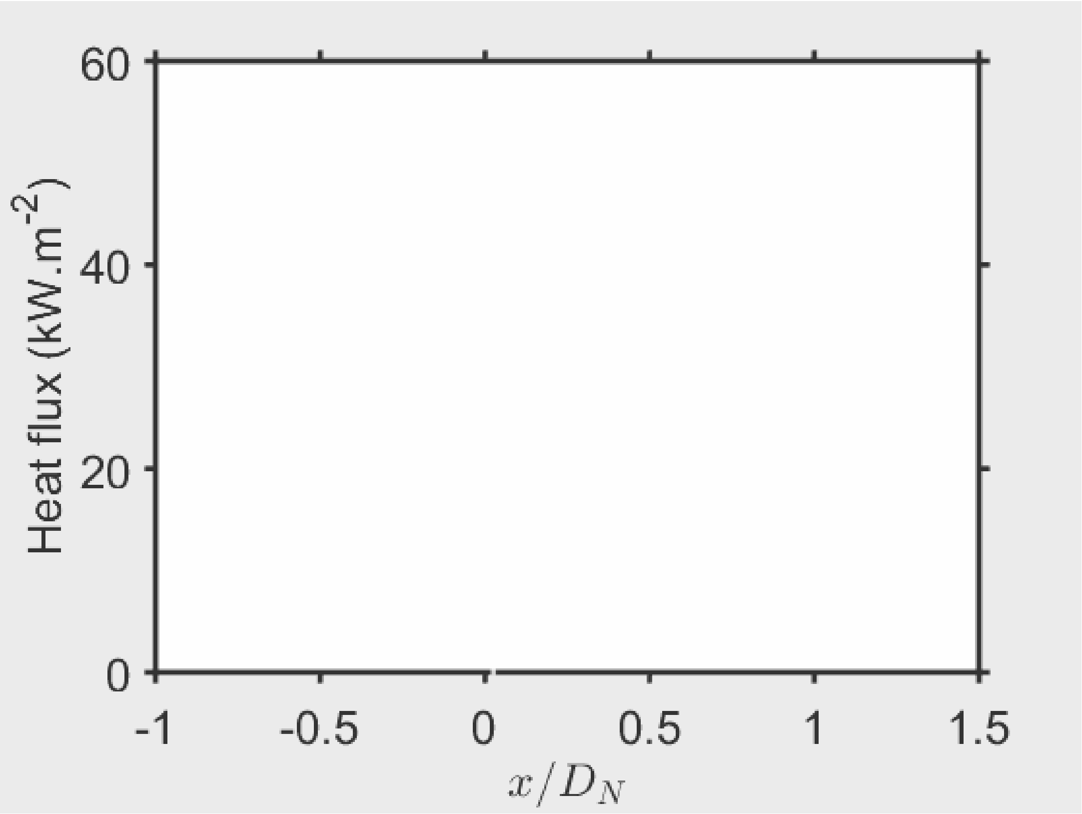

Combustor liner heat flux measurement

- High heat transfer at low liner temperature
- Peak location moves downstream, from *x/D* = 1.8 (*t*=20) to *x/D* = 2.4 (*t*=180)
- Heat transfer at steady state at *t* > 160
- Heat transfer peak is 23 kW/m2 at $x/D_N \approx 2.3$ at steady state
- Increase of heat flux at $0.9 \leq \; x/D_N \leq 2.3$ due to heat release in reacting flow attached to liner wall

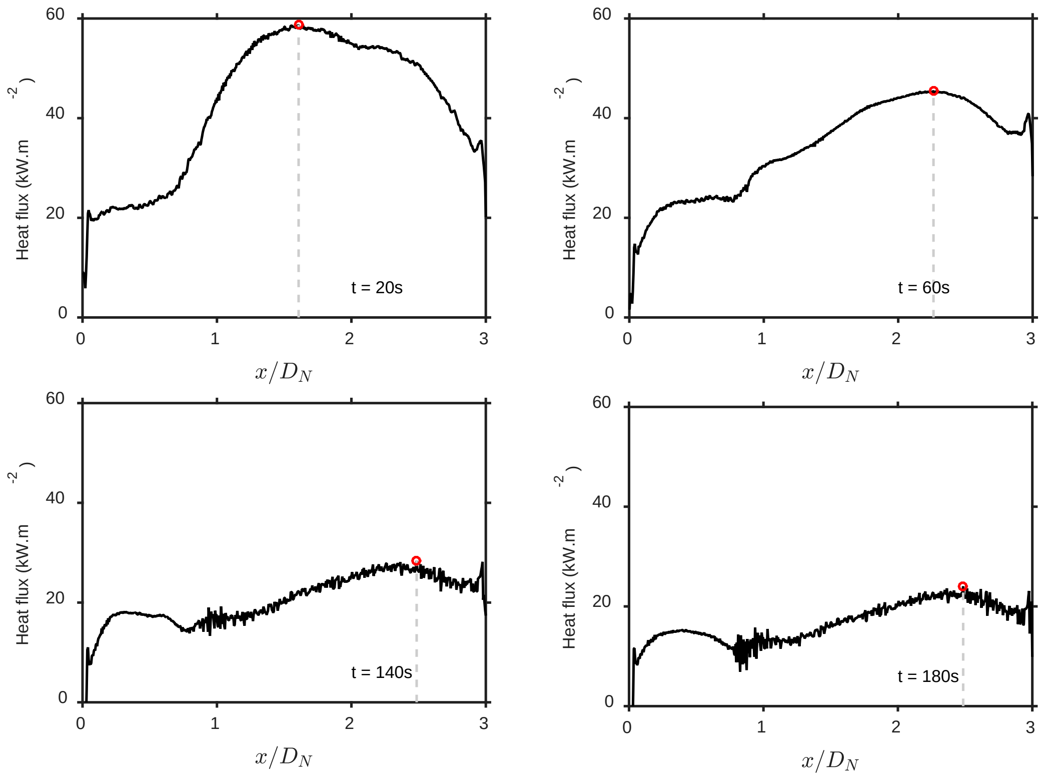

Combustor liner heat flux measurement

- High heat transfer at low liner temperature
- Peak location moves downstream, from *x/D* = 1.8 (*t*=20) to *x/D* = 2.4 (*t*=180)
- Heat transfer at steady state at *t* > 160
- Heat transfer peak is 23 kW/m2 at $x/D_N \approx 2.3$ at steady state
- Increase of heat flux at $0.9 \leq x/D_N \leq 2.3$ due to heat release in reacting flow attached to liner wall

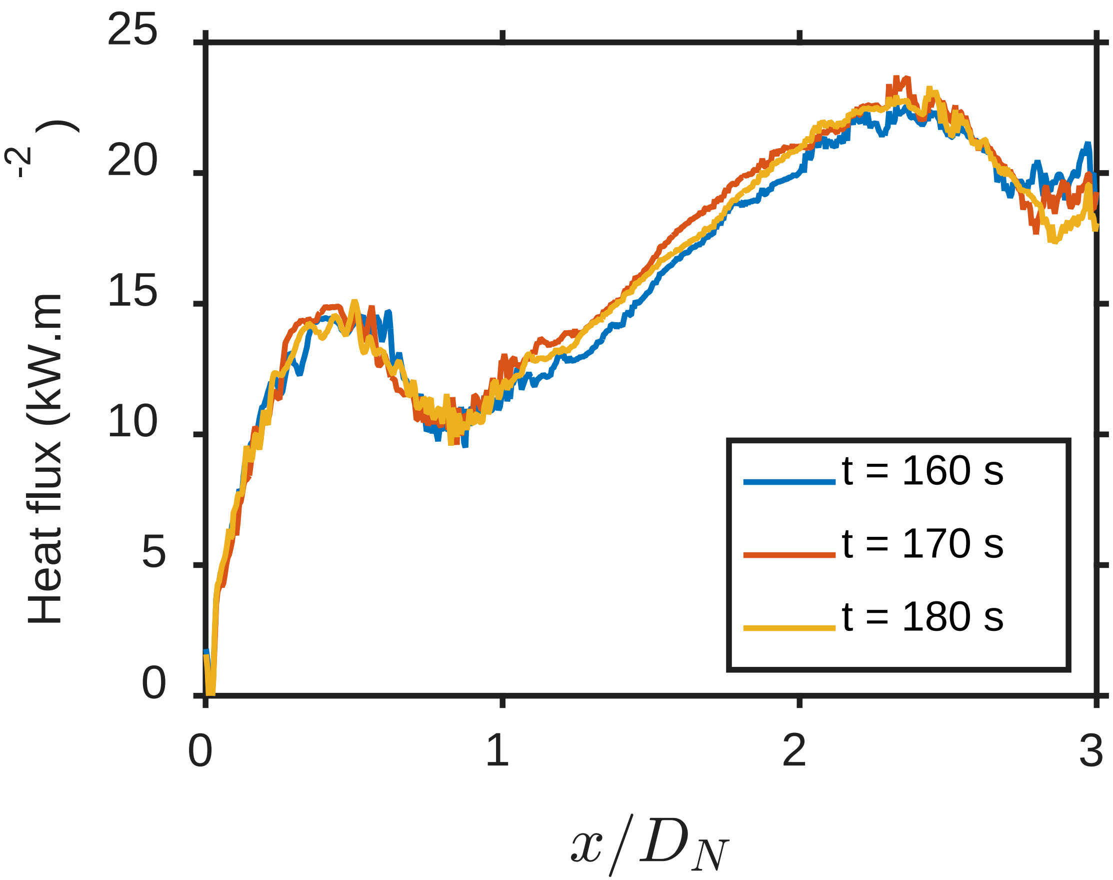

Heat flux axial distribution in time

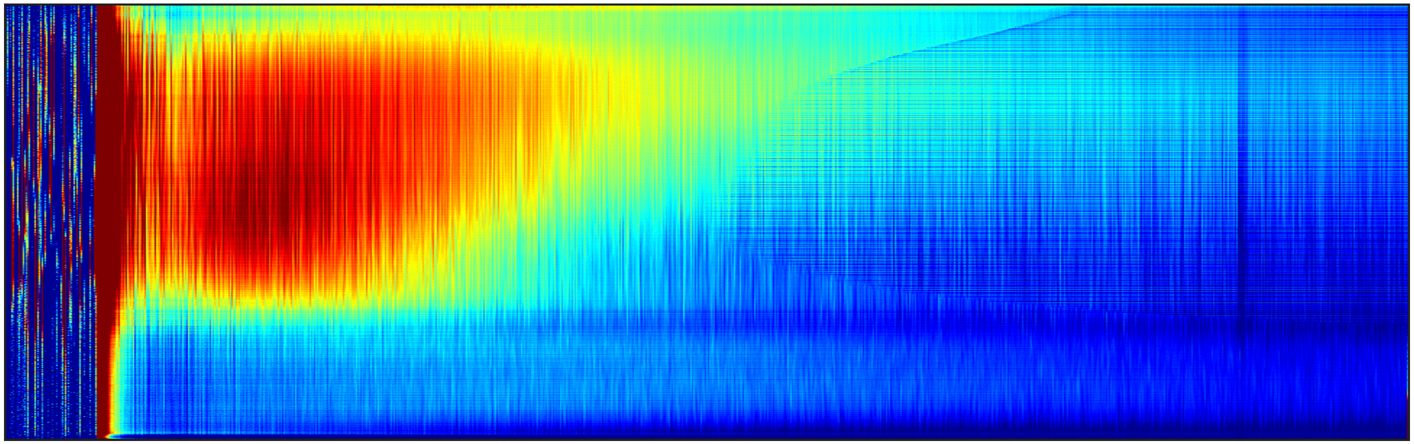

Axial distribution of heat flux on hot side (inner wall) in time

- Initially ($0 < t < 3$ s) peak heat flux reached higher than 200 kW/m^2
- When liner is cold ($t < 80$s), peak heat flux was about 50-60 kW/m^2
- After liner warmed up ($t > 80$ s), heat flux reduces below 40 kW/m^2
- Peak heat load location moved from upstream ($x/D_N = 1.8$) to downstream ($x/D_N = 2.4$)

Reacting Flow Field

2D velocity field measurement with
PIV (Particle Image Velocimetry)
to study swirl flow field structure

PIV experimental setup at combustor rig

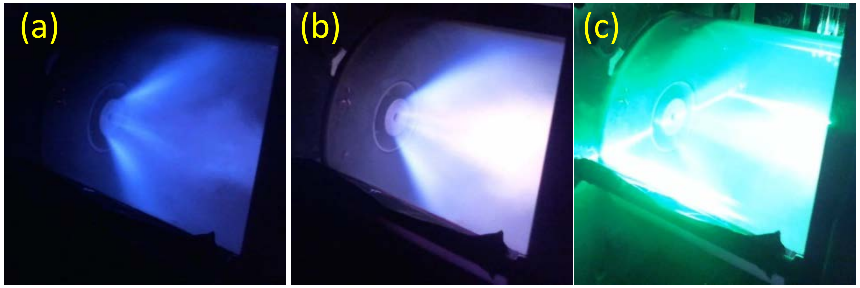

PIV measurement, (a) flame luminosity, (b) seeding particle injection, (c) laser sheet

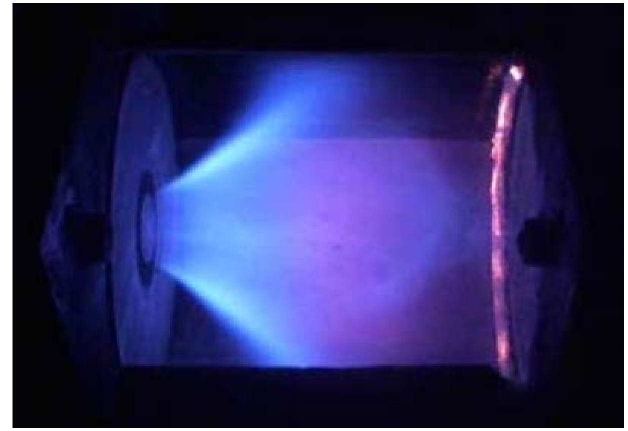

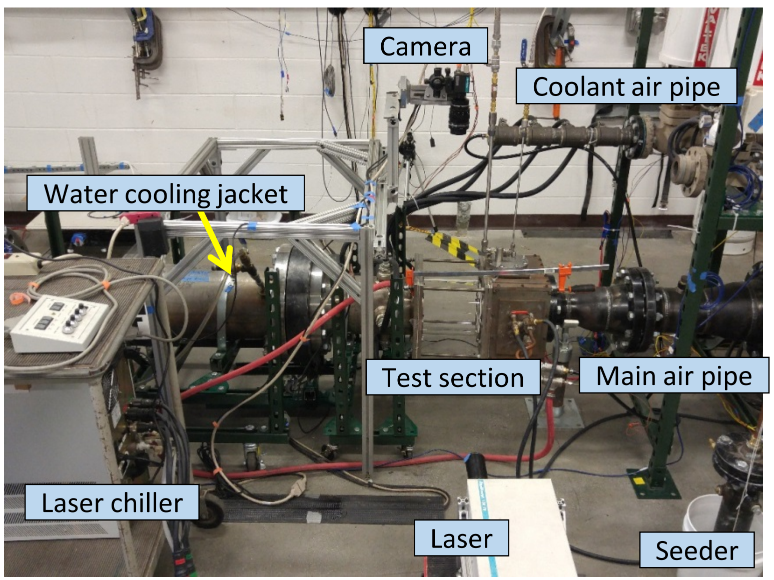

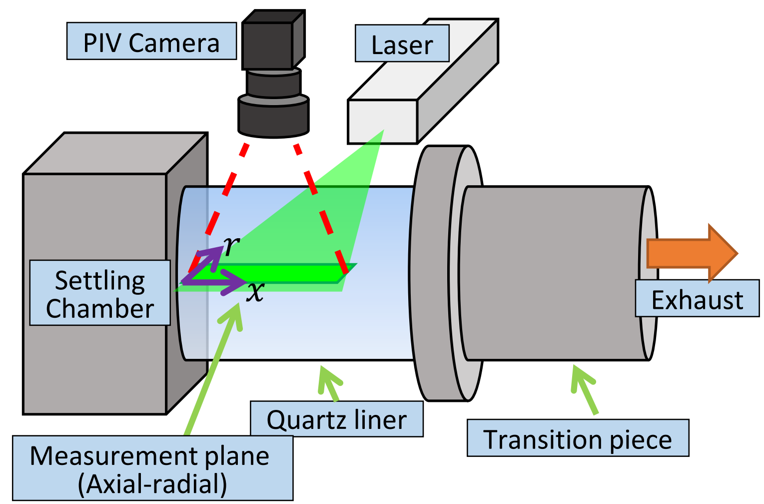

PIV measurement experimental setup at combustor rig

PIV flow field – Non-reacting vs. Reacting

Fixed: Re #: 50,000

Non-reacting | **Reacting (ϕ : 0.65, Pilot: 6%)**

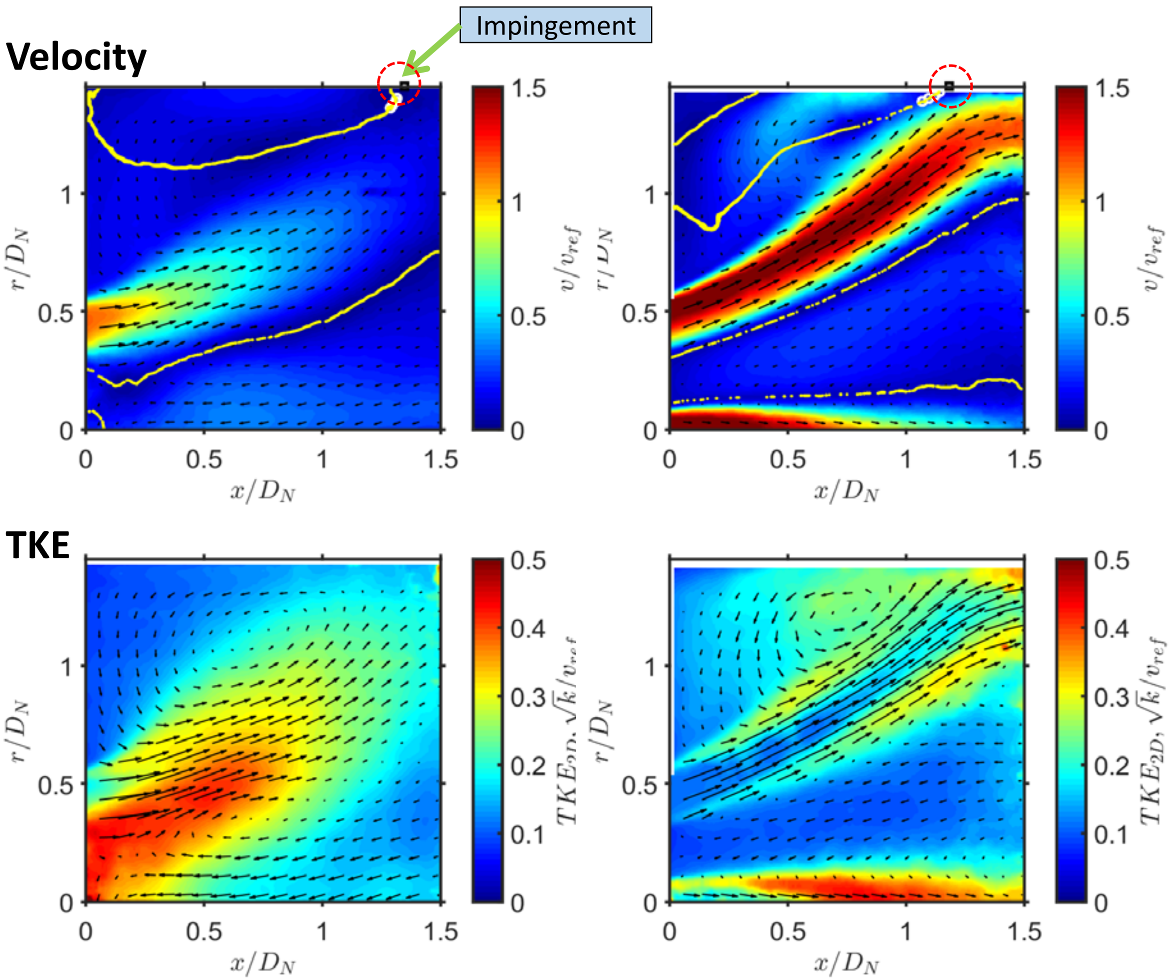

Flow field characteristics in reacting flow are distinctly different from non-reacting flow

- ***Maximum velocity in the jet is higher in reacting flow because of flow energization***
- **High turbulence regions lie on shear layers for reacting case**
- Axial position of **zero axial velocity** at the liner wall indicates **jet impingement location**

Profile comparison of PIV flow fields

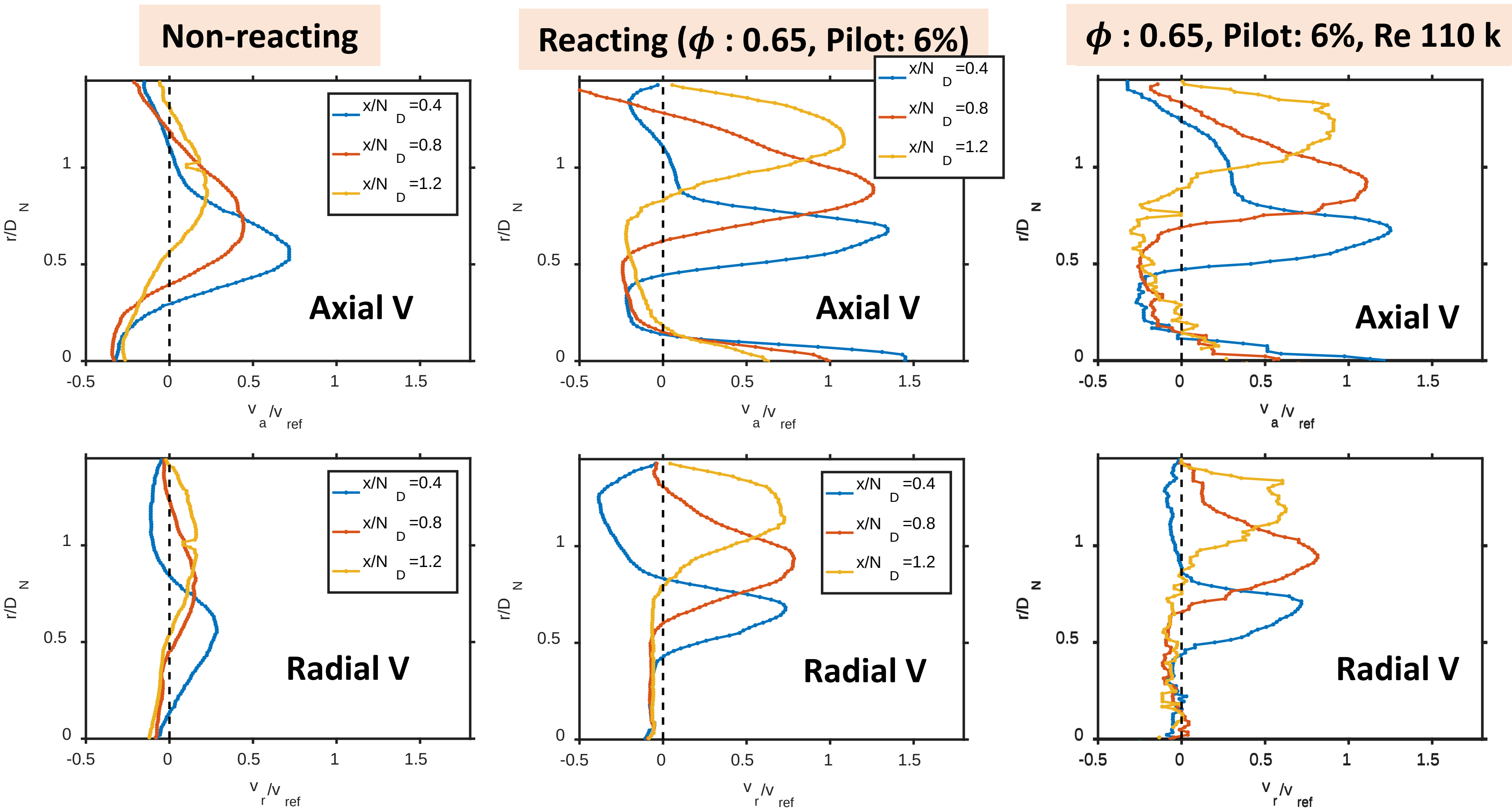

- Main jet in non-reacting decays as it moves downstream
- Self-similarity observed in velocity profiles in reacting flows under different conditions

Impingement locations with different conditions

Impingement locations on the liner wall

Case	Pilot %	ϕ	Re #	x/D_N	Deviation
NR1	-	-	50 k	**1.34**	**-**
NR2	-	-	50 k	**1.32**	**-**
R1	6	0.65	50 k	**1.18**	**+1.9 %**
R2	4	0.65	50 k	**1.23**	**+6.2 %**
R3	0	0.65	50 k	**1.17**	**+1.0 %**
R4	6	0.78	50 k	**1.10**	**-5.0 %**
R5	6	0.55	50 k	**1.01**	**-12.8 %**
R6	6	0.65	75 k	**1.25**	**+7.9%**
R7	6	*0.55*	110 k	**1.17**	**+1.0 %**

For reacting cases:
Mean x/D_N: **1.16**, STD: 0.08 (**7%**)

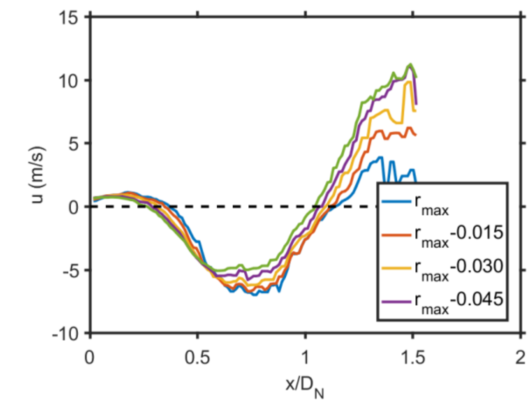

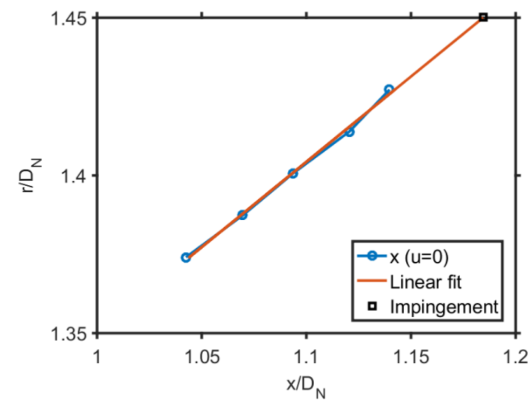

- Impingement location of the flame on the wall is located approximately $x/D_N \sim 1.16$
- Measurement error (alignment, noise, etc.) might have caused minor differences, but **the impingement locations appear consistent for all reacting cases**

2D Flow Temperature

Thermocouple probe scanning measurement on reacting flow

Temperature measurement

- Temperature distribution in 2-D plane of reacting flow for:
  - ✓More accurate **heat transfer** characterization
  - ✓Better understanding of the **combustion process**

- Thermocouple was installed on 2-D linear motorized traversers
- A probe with B type thermocouple was used in the reacting flow
- Connections were protected by insulation casing

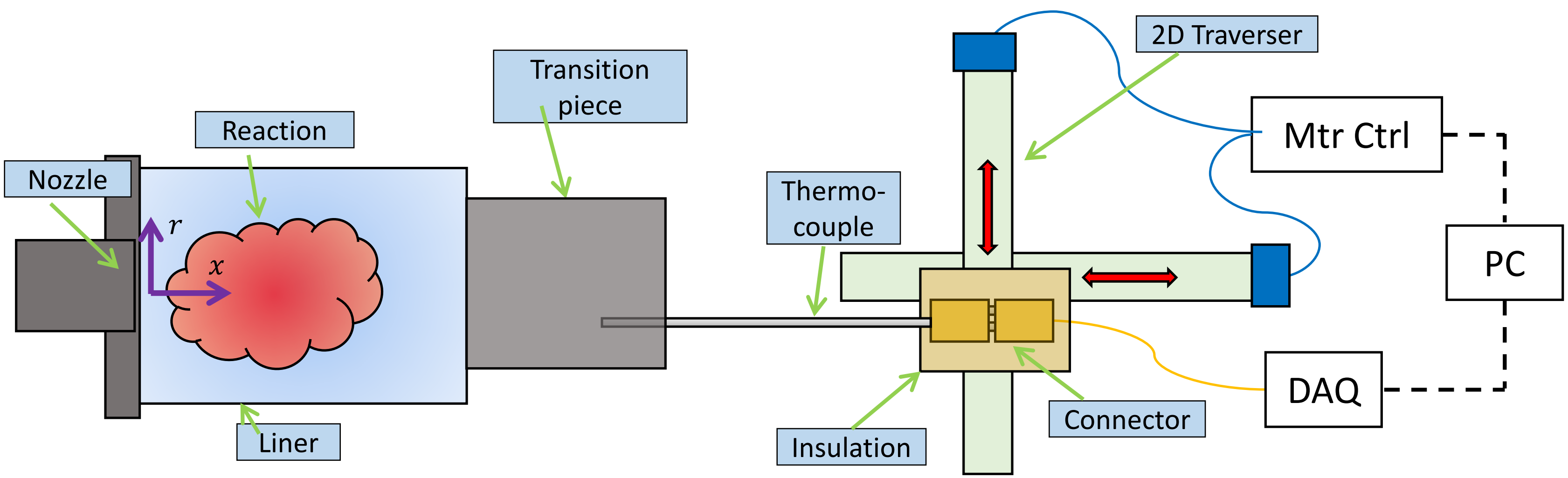

Diagram of temperature mapping setup in reacting flow

Temperature measurement

- Temperature distribution in 2-D plane of reacting flow for:
  - ✓More accurate **heat transfer** characterization
  - ✓Better understanding of the **combustion process**

- Thermocouple was installed on 2-D linear motorized traversers
- A probe with B type thermocouple was used in the reacting flow
- Connections were protected by insulation casing

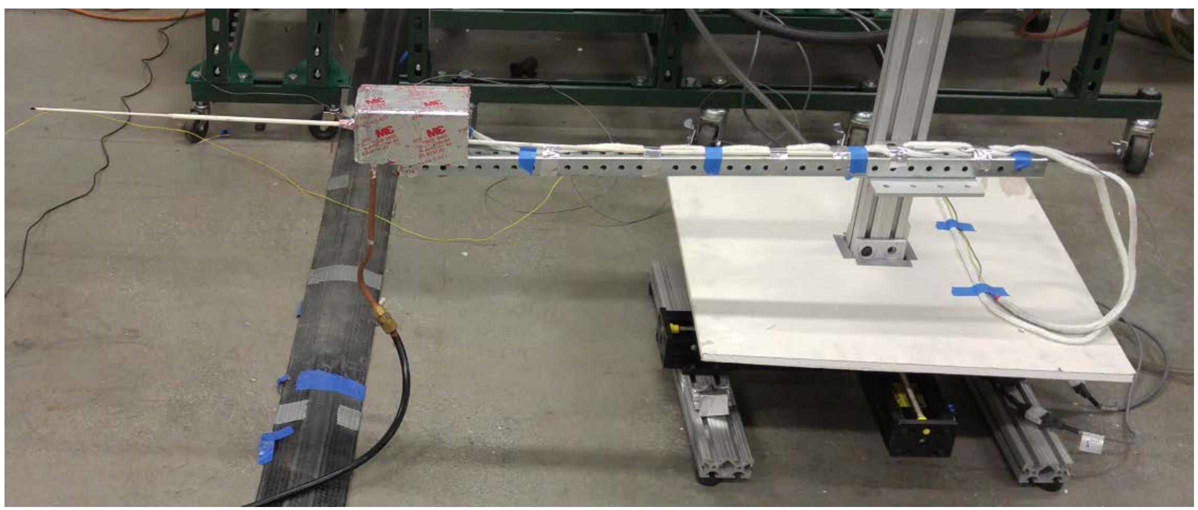

Temperature measurement – Primary zone mapping

Combustor reacting conditions
- Re : 50000
- Equivalence ratio: 0.65
- Pilot fuel ratio: 6%
- Open combustor
  (without transition piece)

TC r-x plane scan setting
- Resolution: r - 5 mm, x - 10 mm
- Number of averaged samples : 3
- Time between samples : 0.5 s
- STD of samples : < 0.5%
- Number of nodes : 20 * 16
- Area : $0 < r_{ND} < 1.36$, $0.14 < x_{ND} < 2.29$

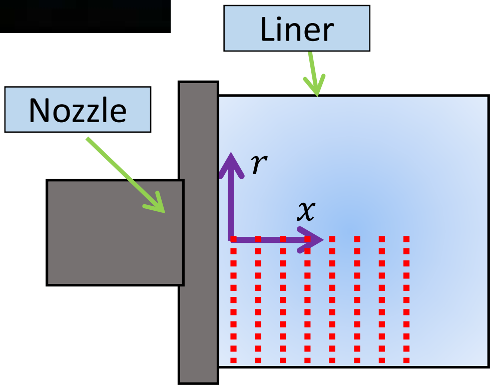

Schematic (top)

Temperature measurement – Primary zone mapping

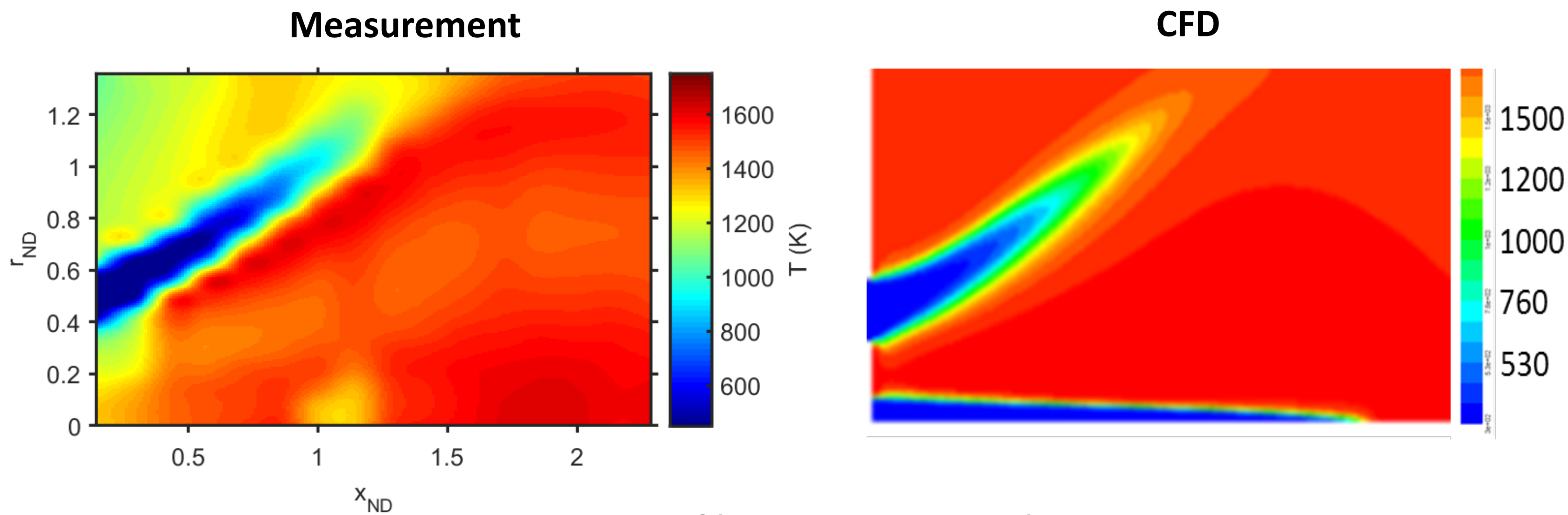

Temperature profiles in reacting combustor

- Highest temperatures were found at two locations
  - ✓ Shear layer between main flame and central recirculation
  - ✓ Center of recirculation zone, downstream of pilot flame
- Lower near wall temperature at $x_{ND} \approx 1.2$ was due to impingement of fresh mixture
- Near wall fluid temperature increases as the attached flow reacts continuously at downstream of impingement location
- Temperature at central recirculation was relatively uniform

Temperature measurement – Axial line scans

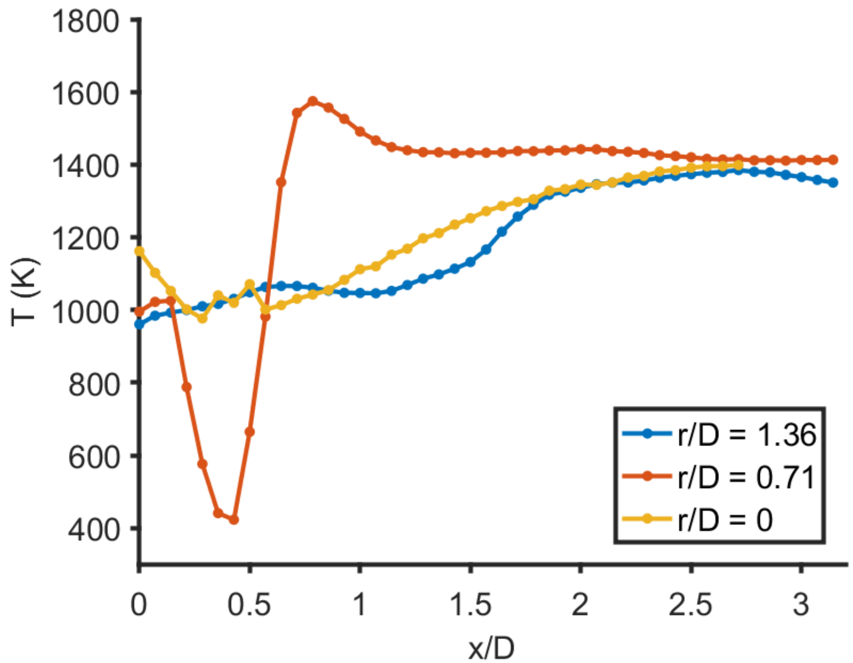

Temperature profiles in axial scanning
Inside combustor liner

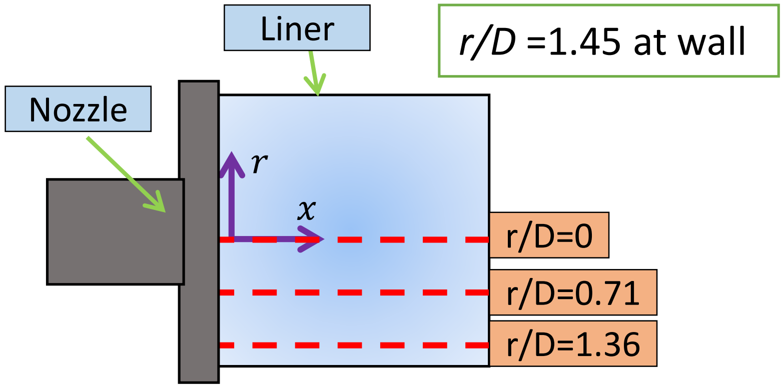

Schematic (top)

Conditions

- Axial resolution: 5 mm (0.0714 D)
- Number of averaged samples : 3
- STD of samples : < 0.5%
- Number of nodes : ~300
- Number of repeat: 2 (1 for r/D = 0)

- Temperature ranged 1000 K to 1500 K except flame jet region
- Maximum and minimum in reacting flame jet region (0.2 < x/D < 1, r/D=0.71) were 1600 K and 400 K (at cold fuel air mixture and flame front)
- Near wall (r/D=1.36) temperature was higher at x/D > 1.7 due to continuous heat release of reacting flow attached on the wall

Flame IR Radiation

Infrared thermographic camera measurement on reacting flow

Infrared radiation of reacting flow in combustor

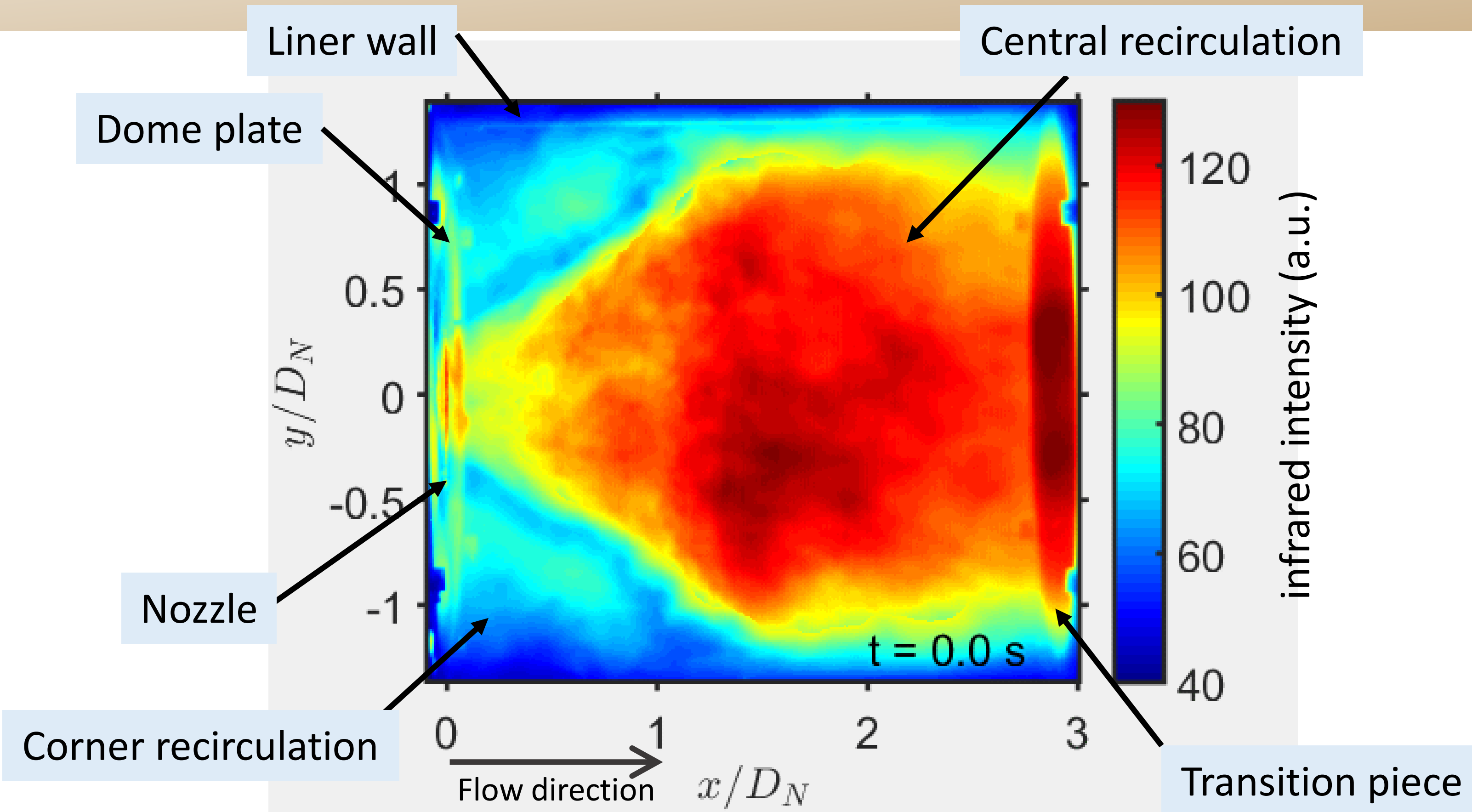

Instantaneous snapshots of flame IR radiation

- 7.5 Hz rate, 60 s duration
- Length scale was normalized with the fuel nozzle diameter, D_N
- Strong radiation around the axis
- Turbulent behavior of the flow was observed

Reconstruction of the flame infrared radiation

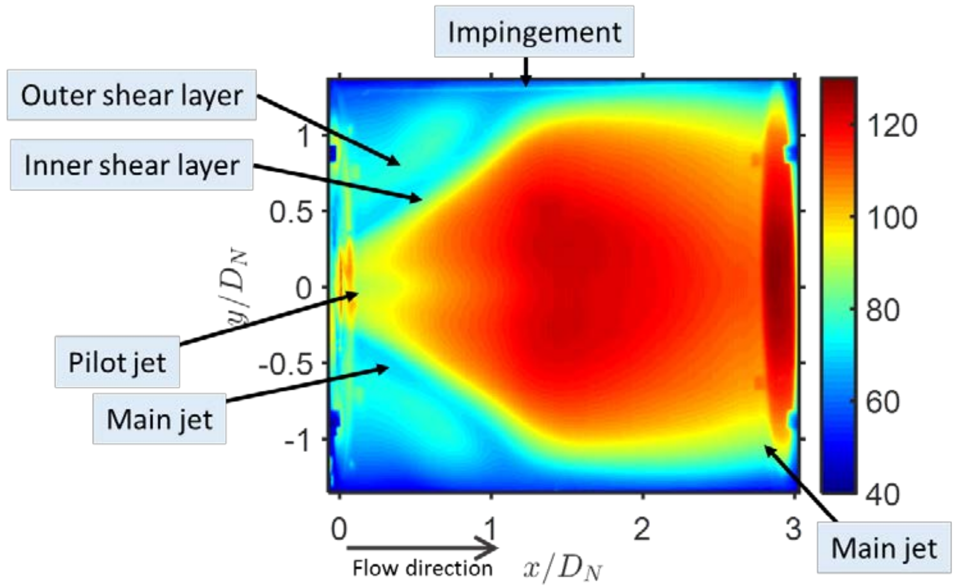

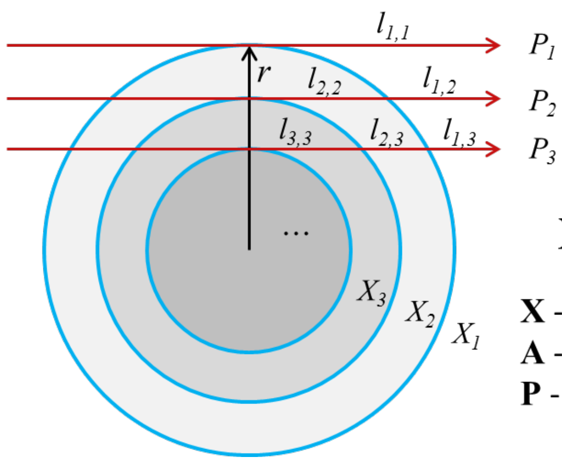

$$\mathbf{X} = \mathbf{A}^{-1}\mathbf{P}$$

X - Distribution
A - Geometry
P - Projection

Averaged flame IR radiant energy density

- Line-of sight averaged Two shear layers were observed (not visible in visible luminosity image)
- High intensity at hot metal surfaces, but not at quartz glass surfaces

Abel transformation

- Line-of sight averaged radiant density projection was observed (left)
- Tomographic inversion for axisymmetric geometry
- Projection images are reconstructed to represent planar distributions

Reconstructed flame infrared radiation

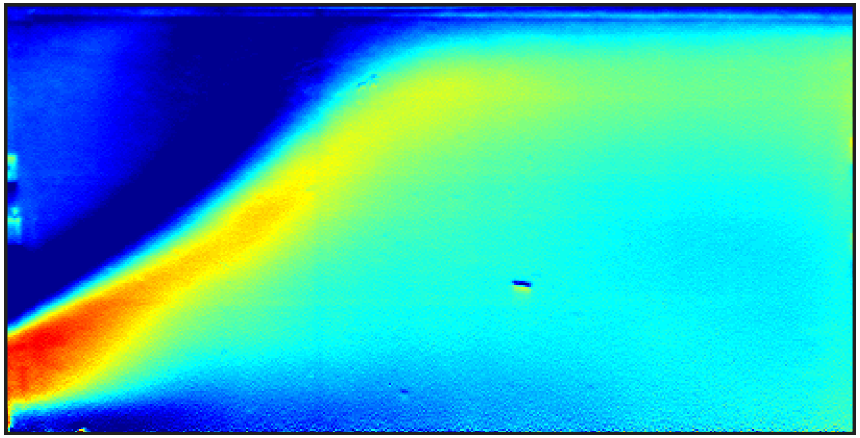

Reconstructed infrared radiant energy density (a.u.).

Infrared radiant energy density in axial-radial plane.

- The inner structures of swirl flame are more distinct.
- Flow structures shown better than the projection.
- Flame front between incoming fresh mixture and central recirculation zone
- The flame front divides the image into two zones
  1) main jet and corner recirculation, 2) central recirculation.
- The highest intensity: near the nozzle
- The lowest intensity : incoming fresh mixture at main jet.

High Speed Imaging

To observe flame features using high speed direct light imaging

High Speed Imaging – Setup

Objective: To observe flame features using high speed direct light imaging

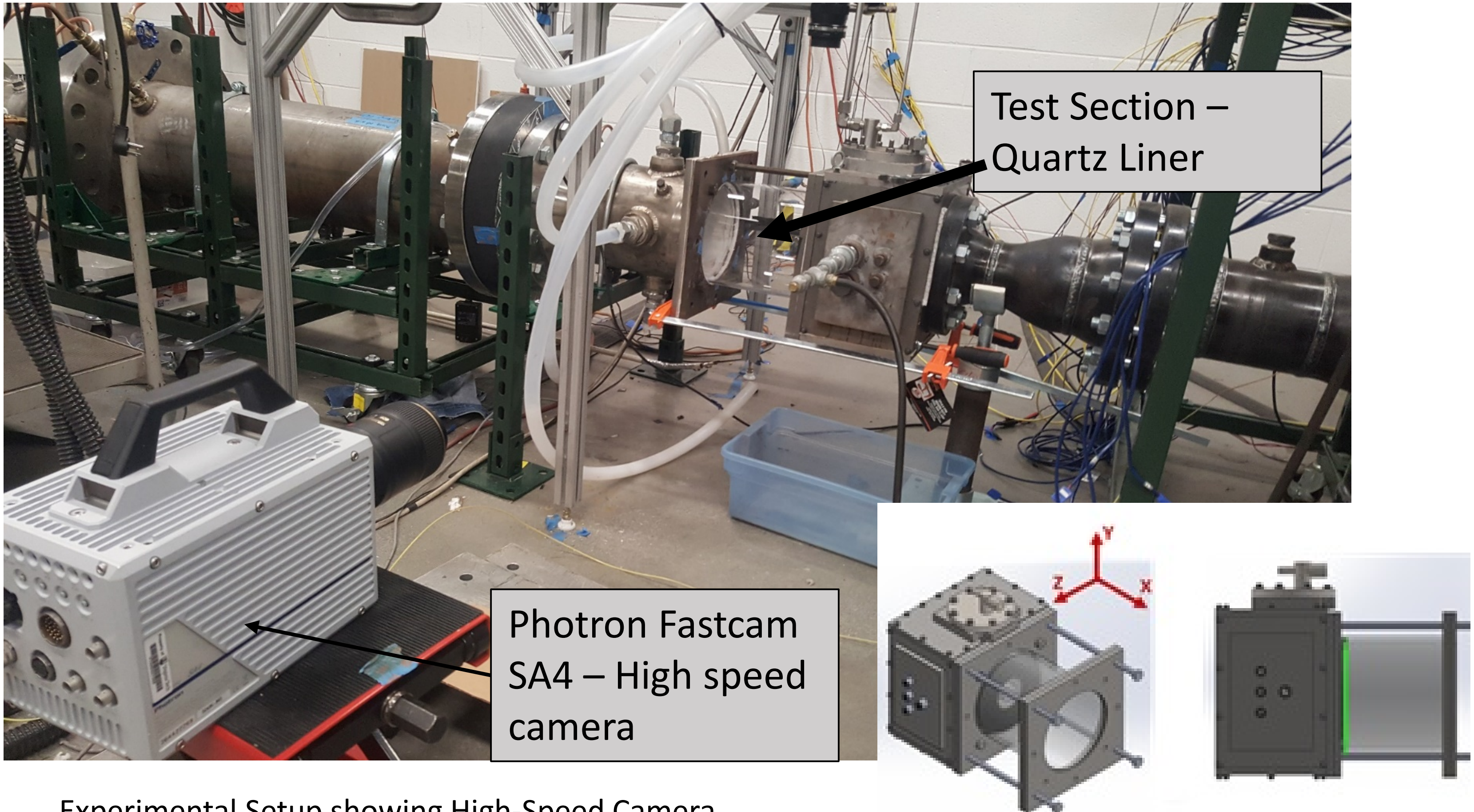

Experimental Setup showing High-Speed Camera

Test Section – Images taken in X-Y plane

High Speed Imaging - Post Processing Methodology

Objective: To observe flame features using high speed direct light imaging

Proper Orthogonal Decomposition (POD) on flame images → Reduced order model give **dominant structures** in the flames as different modes → Temporal information (coefficients) from POD gives information about the **oscillations** in the flame → Observation of **Combustion oscillations**

POD is a statistical tool to decompose time-series data into **low order model**

The **images can be reconstructed** based on the low order model of POD which helps in **separating various fluctuations** observed in the data set.

Spatio-Temporal dynamics of the flame images are **decomposed** into constituent POD modes.

Highest POD mode represent the maximum spatial variance observed. Other POD modes shows spatial variance according to mathematical significance.

Spatial variance in flame images is because of the flame dynamics.

POD Modes - Stable Flame

50K Re | 6% pilot | 0.75 Eq ratio

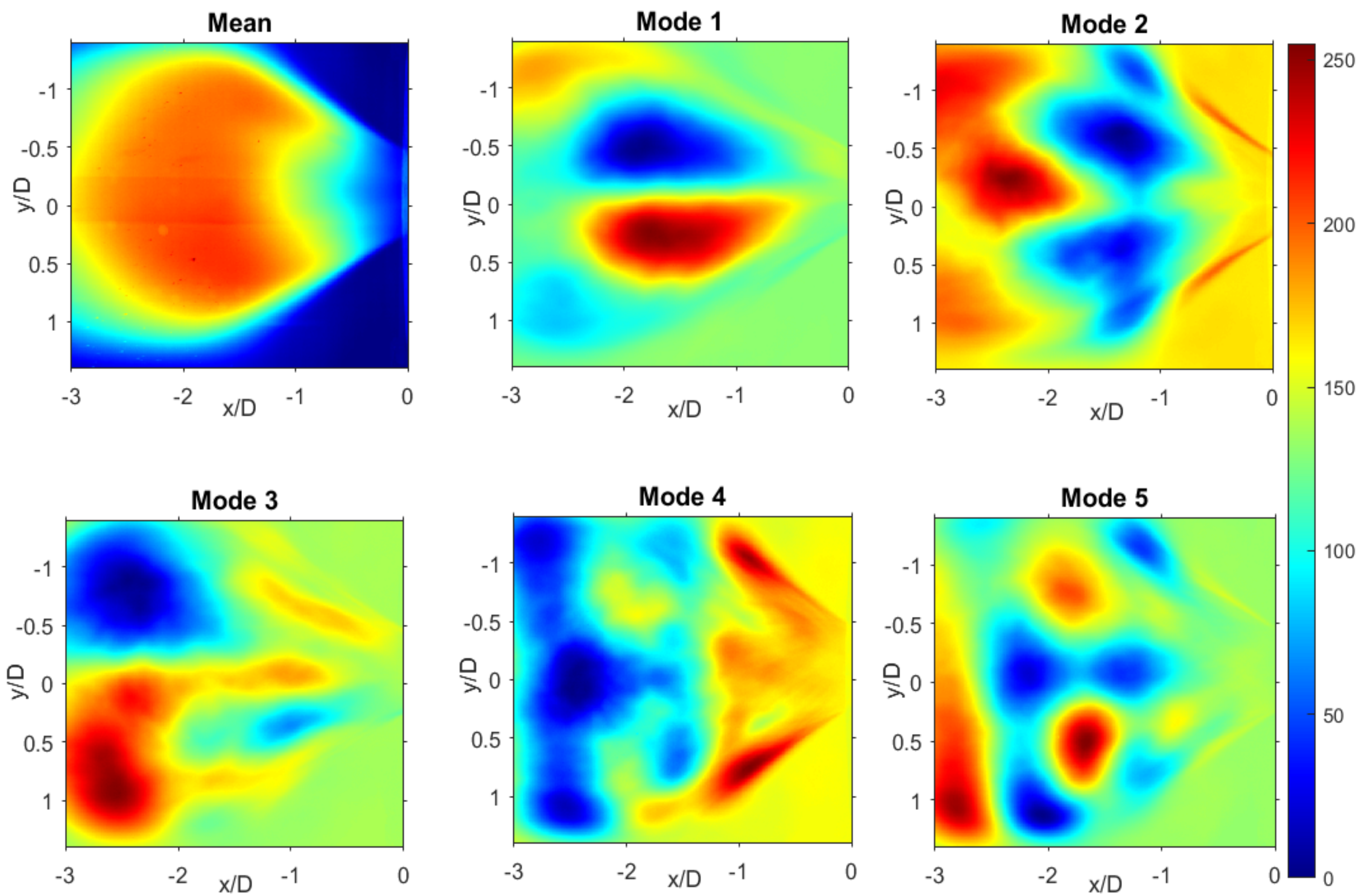

Mean Image and Top 5 POD Modes

POD Time Coefficients and Pressure Measurements similarity

Top POD modes obtained from high speed imaging replicates the pressure PSD (some peaks) below 100Hz

200Hz frequency oscillations are due to coolant air (separate testing has been done to validate)

Mode 2 of POD was used for this plot which corresponds to 5% of energy (mode 1 is 7% for comparison).

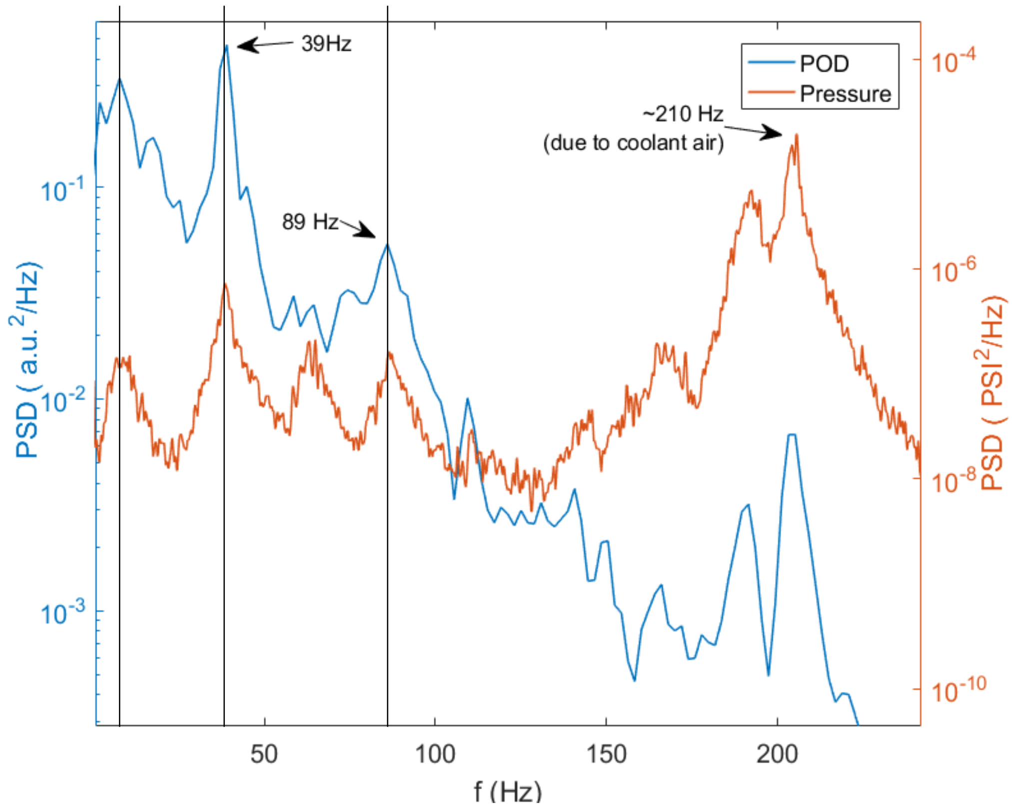

Power Spectral Density of POD Time Coefficient and Pressure Measurement show similar frequency peaks

POD Time Coefficients Comparison - Other Stable Cases

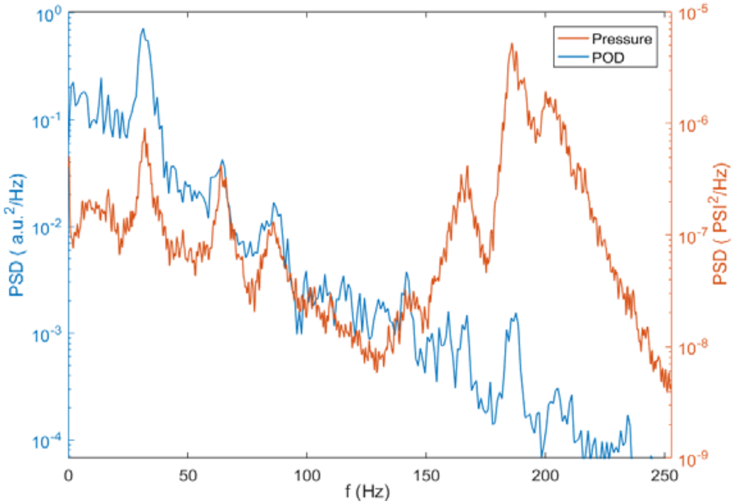

50K Re | 6% pilot | 0.65 Eq ratio

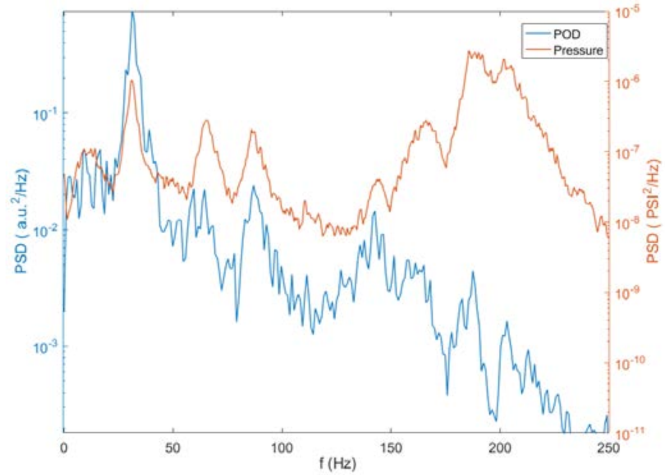

50K Re | 0% pilot | 0.65 Eq ratio

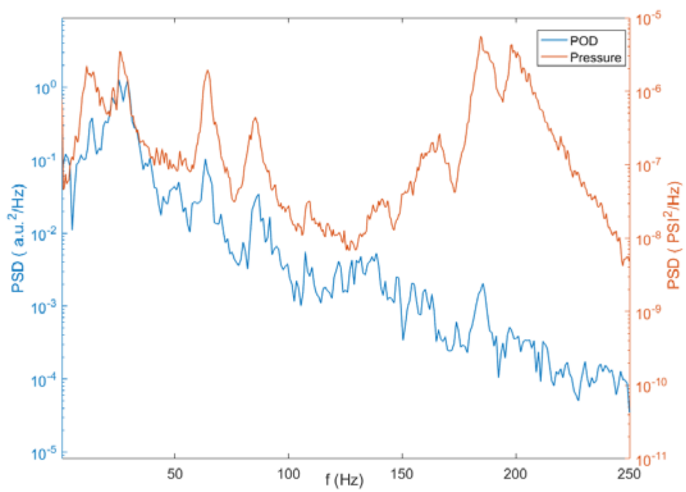

50K Re | 4% pilot | 0.65 Eq ratio

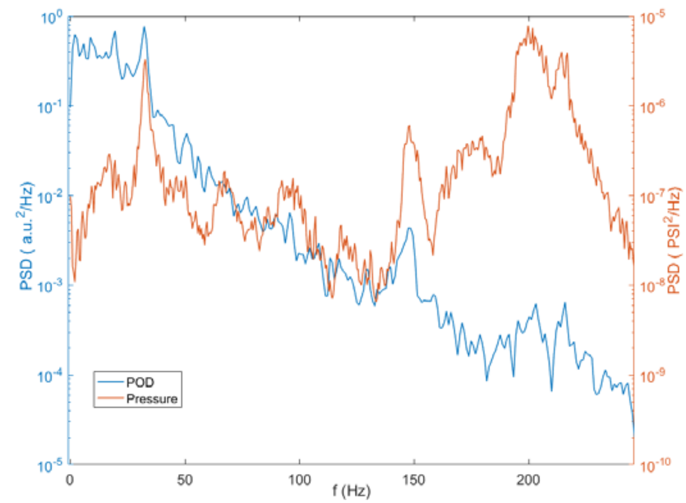

75K Re | 6% pilot | 0.65 Eq ratio

High Speed Imaging - Near Blowout Oscillations

Objective: To observe flame features and oscillations using high speed imaging

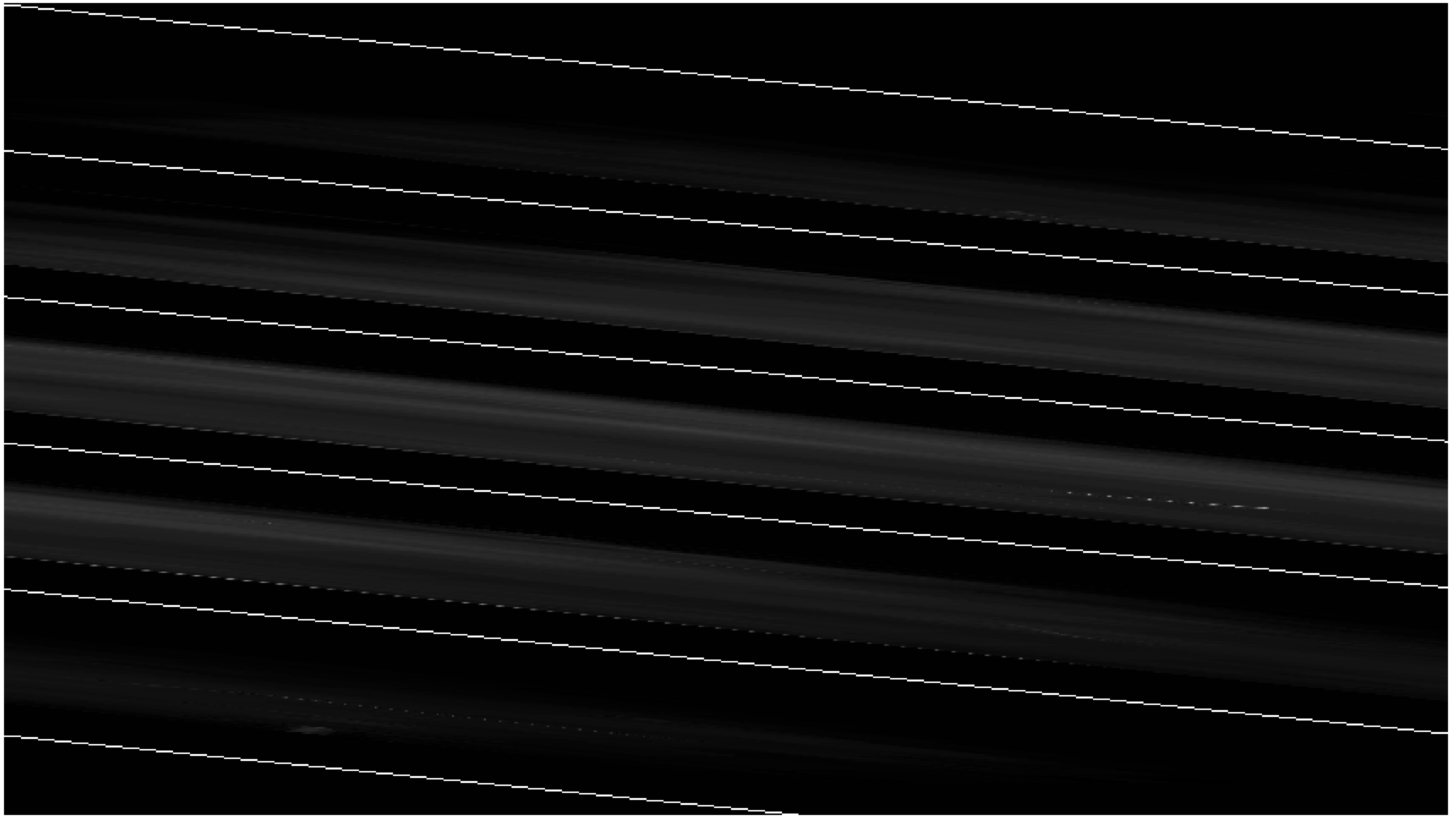

Animation shows high Speed Images acquired during near blowout Oscillations. The objective is to study these oscillations using the snapshots obtained from high speed imaging

Near Blowout Oscillations - POD Modes

High Speed images were obtained at 500 Hz

POD Modes indicate flame extinction and re-ignition

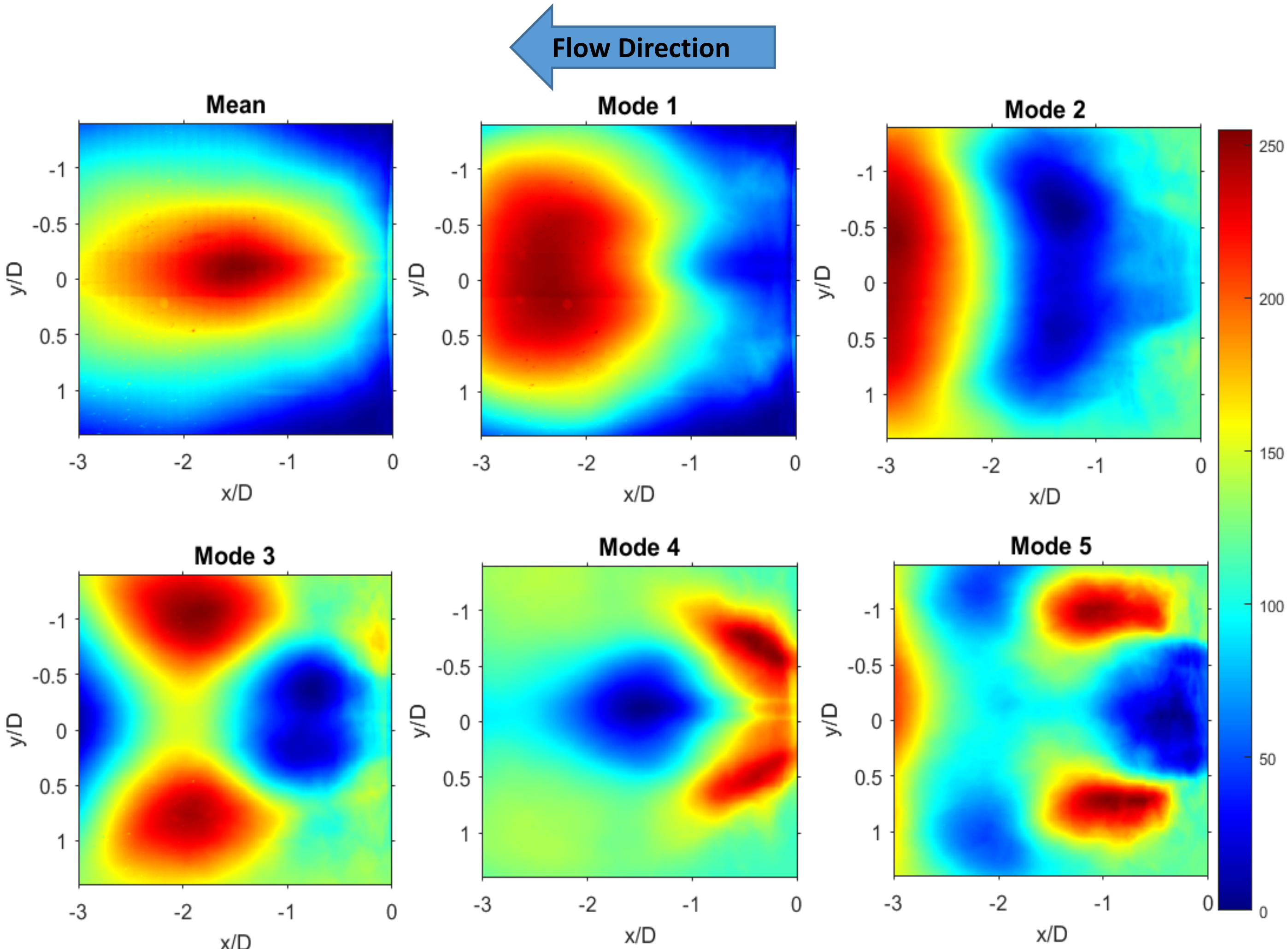

POD Modes - Near Blowout Oscillations

POD Time Coefficients and Pressure Measurements similarity

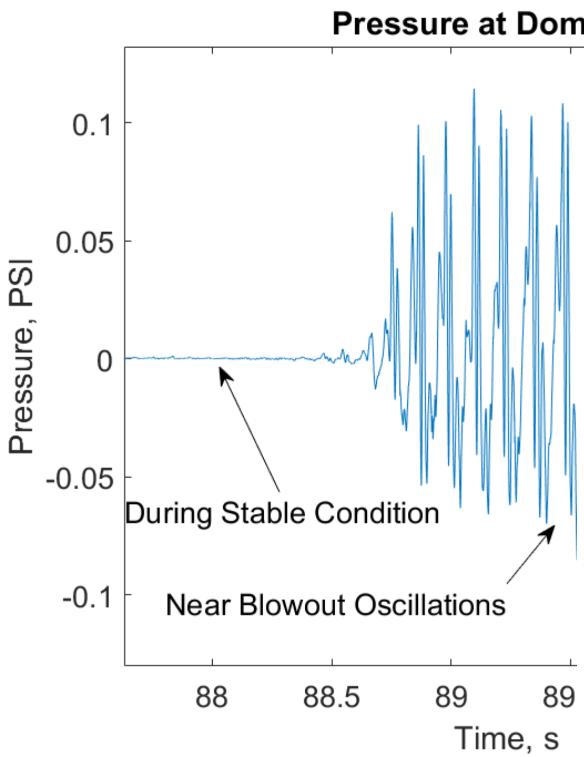

POD was able to replicate the same frequencies as that of pressure fluctuations - **7.8 Hz**

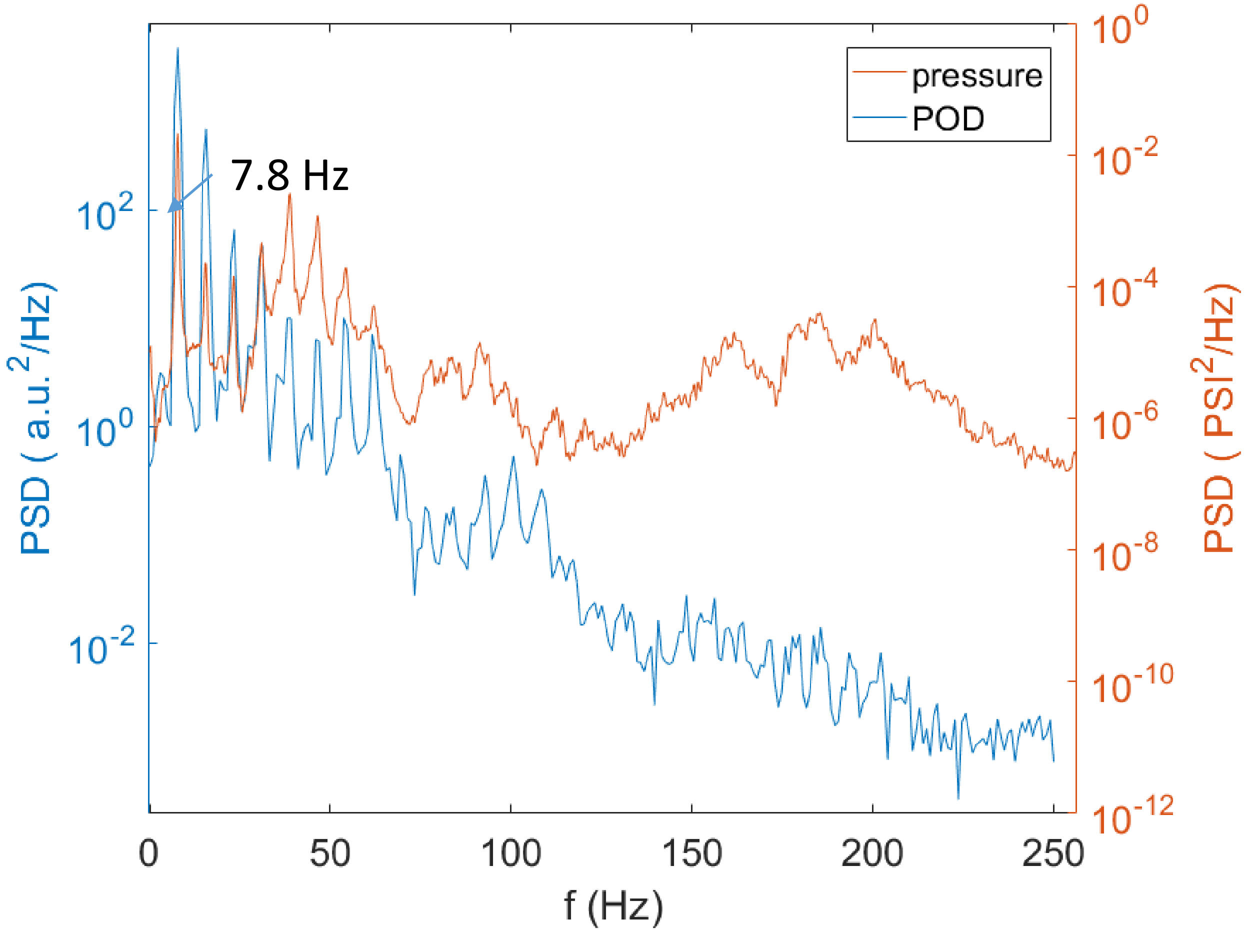

Power Spectral Density of POD and Pressure

POD Reconstruction Example

Instantaneous Snapshots are not sufficient to understand the flame structure.

POD reconstruction shows statistically dominant flame structures

Near Blowout - POD Reconstruction

Flow Direction

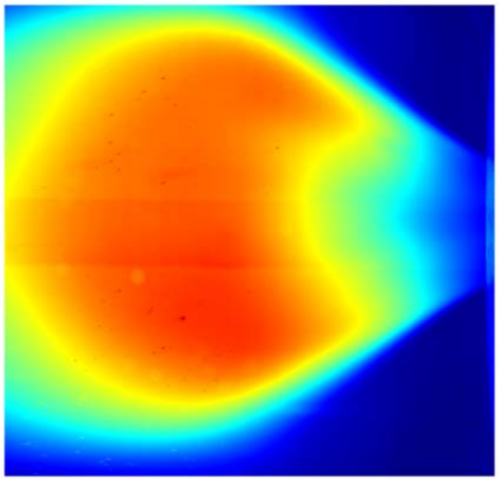

Mean Image of a Stable case

Compared to stable case, the flam spread even in the corner recirculation zone

The Flame oscillation observed here correspond to the same 7.8 Hz observed in the pressure measurement

VirginiaTech Invent the Future®

APPL

Liner Wall Heat Transfer During Oscillations

Heat load on liner wall During Near Blowout Oscillations

Heat Flux Oscillations - Same as POD Temporal Coefficients

Transient Heat load measurements using IR-Thermography.

High magnitude fluctuations in heat flux were observed

Heat Flux Oscillations - Same as POD Temporal Coefficients

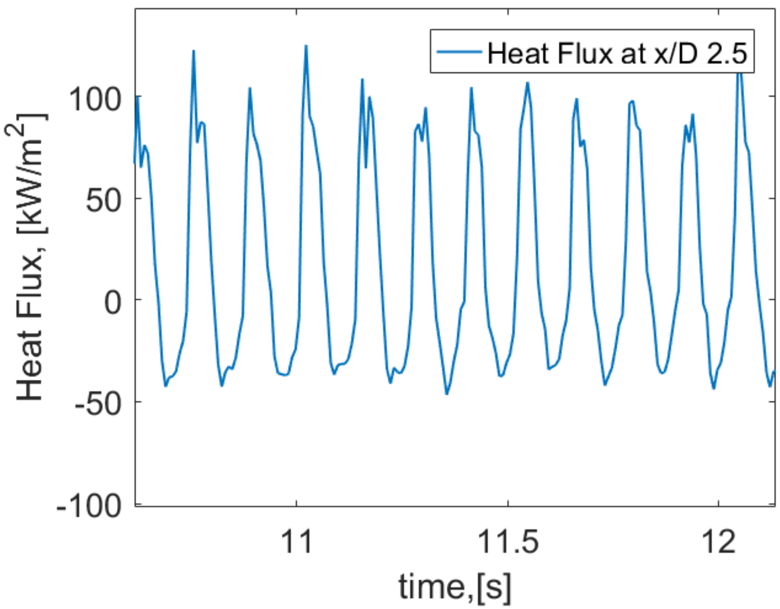

Time Trace of Heat Flux

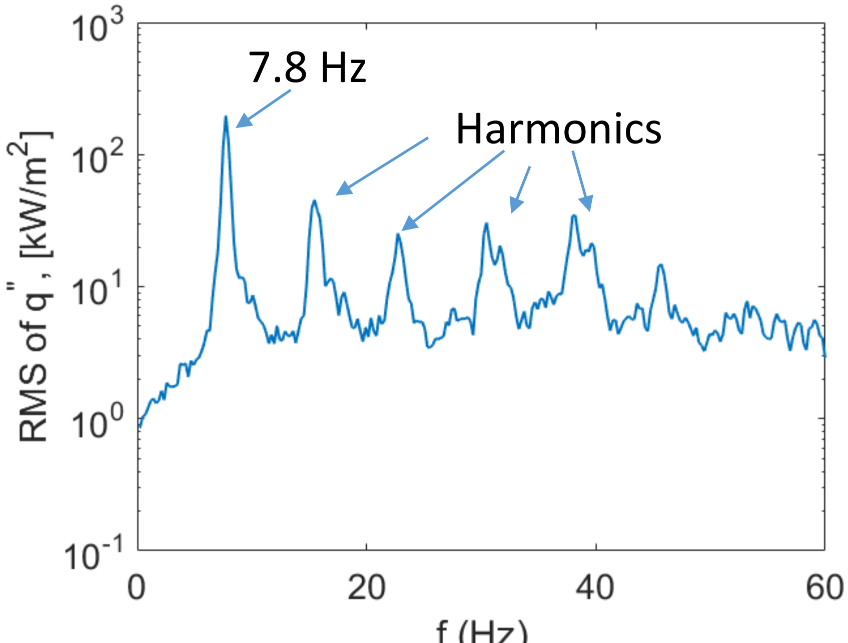

Power Spectral Density of Heat Flux

Amplitude of Heat Flux fluctuation is huge

Heat Flux plotted at x/D_N 2.5

Spectra shows **7.8 Hz frequency** same as that of pressure oscillations and POD Temporal Coefficients.

Summary

Swirl flow field and heat transfer measurement

- Flow field structure and impingement locations were not sensitive to combustor operating parameters
- Temperature field inside combustor was measured in combustor primary zone
- Axial distribution of hot side heat flux on combustor liner wall was measured
- Moving maximum heat flux location was observed
- Feasibility of IR thermographic camera to measure thermal properties of turbulent reacting flows was demonstrated.

High Speed Imaging and Heat Transfer – Unstable combustion

- POD on High Speed imaging: Reconstruction and Phase averaging gave insight to flame oscillations
- Heat Transfer during near blowout oscillations showed huge fluctuation in liner heat transfer.

Project Accomplishments

- Development of optically accessible combustion test rig.
- Characterization of liner wall heat transfer and flow field in non – reacting conditions.
- Development of heat transfer technique for liner wall heat transfer in reacting conditions.
- Flow field characterization using PIV in reacting conditions.
- RANS based simulations with FGM model was able to predict combustor flow field numerically
- Liner wall heat transfer in reacting condition.
- Demonstration of IR flame radiation measurements.
- Direct flame temperature measurements.
- Liner wall heat transfer during instabilities.
- Study of flame structures using high speed imaging.

Publications

1. <u>**Kedukodi, S**</u>., Ekkad, S., Moon, H K., Srinivasan, R., Kim, Y., 'Numerical investigation of effect of geometry changes in a model combustor on swirl dominated flow and heat transfer', Proceedings of ASME Turbo Expo 2015 (Montreal, Canada), No. GT2015-43035
2. **DG Ramirez,** V Kumar, SV Ekkad, D Tafti, Y Kim, HK Moon, R Srinivasan, " Flow field and Liner Heat Transfer for a Model Annular Combustor Equipped with Radial Swirlers"
3. **D Gomez-Ramirez**, D Dilip, BV Ravi, S Deshpande, J Pandit, SV Ekkad et al., "Combustor Heat Shield Impingement Cooling and its Effect on Liner Convective Heat Transfer for a Model Annular Combustor With Radial Swirlers", ASME Turbo Expo 2015
4. <u>**Kedukodi, S**</u>., Ekkad, S., 'Effect of downstream contraction on liner heat transfer in a gas turbine combustor swirl flow', ASME Gas Turbine India Conference 2015, No. GTINDIA2015-1206 **(Recommended for Journal and Honors)**
5. **D Gomez-Ramirez**, SV Ekkad, BY Lattimer, HK Moon, Y Kim, R Srinivasan., "Separation of Radiative and Convective Wall Heat Fluxes Using Thermal Infrared Measurements Applied to Flame Impingement ", ASME IMECE 2015
6. <u>**Kedukodi, S**</u>., Ramirez, DG., Ekkad, S., Moon, H K., Srinivasan, R., Kim, Y., 'Analysis on impact of turbulence parameters on isothermal gas turbine combustor flows', ASME 2016 Summer Heat Transfer Conference, No. HT2016-7134
7. **Ramirez, DG.,** <u>Kedukodi, S</u>., Gadiraju, S., Ekkad, S et al., 'Gas turbine combustor rig development and initial observations at cold and reacting conditions', Proceedings of ASME Turbo Expo 2016, No. GT2016-57825
8. **D Gomez-Ramirez**., "Heat Transfer and Flow Measurements in an Atmospheric Lean Pre-Mixed Combustor". PhD Dissertation
9. Gomez-Ramirez, David, et al. "Investigation of isothermal convective heat transfer in an optical combustor with a low-emissions swirl fuel nozzle." *Applied Thermal Engineering* 114 (2017): 65-76
10. **Gomez-Ramirez, David**, et al. "Isothermal coherent structures and turbulent flow produced by a gas turbine combustor lean pre-mixed swirl fuel nozzle." *Experimental Thermal and Fluid Science*81 (2017): 187-201.

Publications

11. **Park, S**. , Gomez-Ramirez, D., Gadiraju, S., Kedukodi, S., Ekkad, S. V., Moon, H.-K., Kim, Y., and Srinivasan, R., "Flow Field and Wall Temperature Measurements for Reacting Flow in a Lean Premixed Swirl Stabilized Can Combustor", ASME Turbo Expo 2017: Turbomachinery Technical Conference and Exposition, American Society of Mechanical Engineers, 2017. GT2017-64837
12. **Kedukodi, S.,** Park, S. , Gadiraju, S., , Ekkad, S. V., Kim, Y., and Srinivasan, R., "Numerical and Experimental Investigations for Flow Fields Under Non-Reacting and Reacting Conditions Through a Lean Premixed Fuel Nozzle", ASME Turbo Expo 2017: Turbomachinery Technical Conference and Exposition, American Society of Mechanical Engineers, 2017. GT2017-64911
13. **Gadiraju, S.,** Park, S. , Gomez-Ramirez, D., Ekkad, S. V., Lowe, K. T., Moon, H.-K., Srinivasan, R., and Kim, Y., "Application of Proper Orthogonal Decomposition to High Speed Imaging for the Study of Combustion Oscillations", ASME Turbo Expo 2017: Turbomachinery Technical Conference and Exposition, American Society of Mechanical Engineers, 2017. GT2017-64602
14. **Suhyeon Park** and Srinath Ekkad, "Flame infrared radiation measurement at a model gas turbine combustor", The 14th International Workshop on Advanced Infrared Technology and Applications, Quebec, Canada, 2017

Publications under review

1. "Characterization of Heat Load on the Liner Walls during Near Blowout Instabilities", SciTech 2018.
2. "Flow Temperature Measurement of Lean Premixed Swirl Stabilized Combustor Under Reacting Condition", SciTech 2018
3. "Fuel Interchangeability Effects On The Lean Blowout For A Lean Premixed Swirl Stabilized Fuel Nozzle", Turbo Expo 2018
4. "Effects Of Reacting Conditions On Flow Fields In A Swirl Stabilized Lean Premixed Can Combustor", Turbo Expo 2018

Acknowledgements

Dr. Srinath Ekkad
Dr. Todd Lowe
Dr. Jaideep Pandit

Dr. David Gomez-Ramirez
Dr. Sandeep Kedukodi
Dr. Prashant Singh
Yongbin Ji

Robin Ames (DOE, NETL)
Hee-Koo Moon, Yong Kim, Ram Srinivasan, Fred Liberatore (Solar Turbines Inc.)

Thank you!

Sensitivity of POD modes on the Ensemble chosen

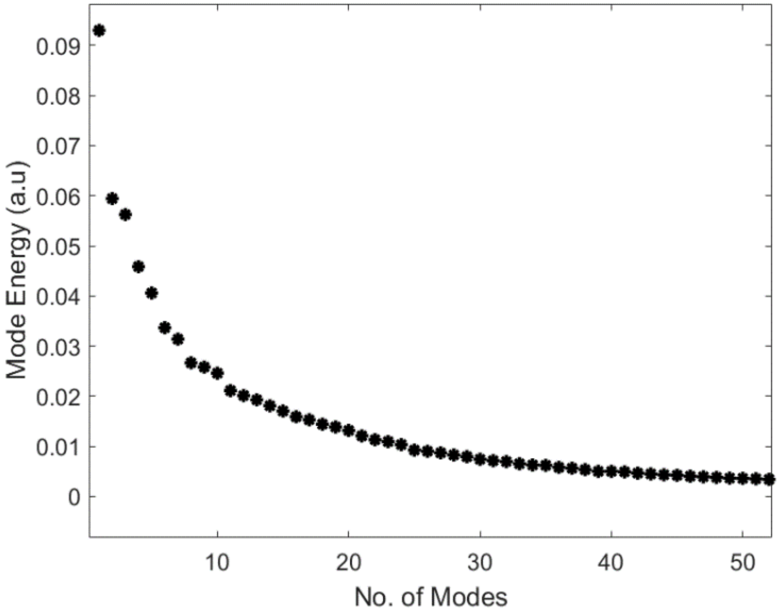

Sensitivity analysis was performed to check the ensemble dependency

Two random ensembles A and B chosen from actual data set and POD was applied

A correlation coefficient is defined as

$$E(I) = \sqrt{\left|\varphi_A^I \cdot \varphi_B^I\right|}$$

Top few modes have most of the energy

First few modes are ensemble independent

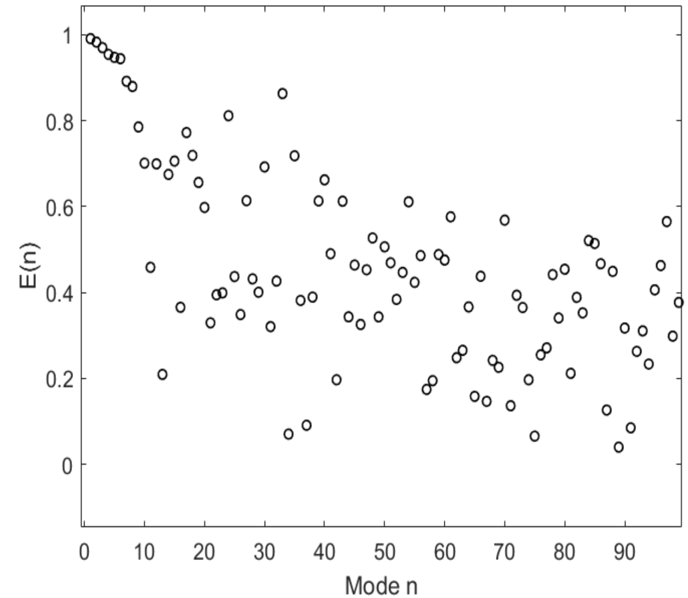

Proper Orthogonal Decomposition - Snapshot Method

Arrange fluctuating part of images for the N snapshots as:

$$X = [x^1\ x^2 \ldots .\ x^N] = \begin{bmatrix} x_1^1 & \cdots & x_1^N \\ \vdots & \ddots & \vdots \\ x_{mn}^1 & \cdots & x_{mn}^N \end{bmatrix}$$

Calculate the covariance as:

$$C = X^T X$$

C is a symmetric matrix and the Eigen value problem can be solved as:

$$C A^i = \lambda^i A^i$$

Eigen Vectors are representative of POD modes

While Eigen values are representation of POD Mode energy

$$\lambda_1 > \lambda_2 > \lambda_3 > \cdots . > \lambda_n = 0$$

POD modes are now found as:

$$\varphi^i = \frac{\sum_{n=1}^{N} A_n^i x^n}{\left\|\sum_{n=1}^{N} A_n^i x^n\right\|}$$

With POD modes arranged as:

$$[\varphi^1\ \varphi^2 \ldots \ldots \varphi^N]$$

POD coefficients a^i can be found for the snapshot i as:

$$a^i = [\varphi^1\ \varphi^2 \ldots \ldots \varphi^N]^T x^n$$

A snapshot (fluctuating part) can be reconstructed as:

$$X_{n,Rec} = \sum_{i=1}^{N} \varphi^i\ a_n^i$$